Electronic Supplementary Material (ESI) for Chemical Communications.

Supporting Information for:

A $Ni(COD)_2$-Free Approach for the Synthesis of High Surface Area Porous Aromatic Frameworks

Anthony J. Porath, Malsha A. Hettiarachchi, Shuxiao Li, and James R. Bour*

Wayne State University, Department of Chemistry, Detroit, Michigan, USA.

Table of Contents

1. General Information

NMR spectra was obtained on an Agilent MR-400 MHz (400 MHz for ^{1}H) and an Agilent DD2-600 MHz (600 MHz for ^{1}H) spectrometer. ^{1}H NMR chemical shifts are reported in parts per million (ppm) relative to tetramethylsilane (TMS) with sample residual solvent peak used as an internal reference. Abbreviations used to report the NMR data: br, broad; s, singlet; d, doublet; t, triplet; q, quartet; dd, doublet of doublets; m, multiplet. Elemental analyses were performed by Midwest Microlab, Inc. located in Indianapolis, Indiana, USA. Combustion aids were used in the analysis of polymers **P-2** through **P-6**. SEM micrographs were performed on a JSM-7600F field emission scanning electron microscope. FTIR analysis was performed on an Agilent Cary-620 FTIR with a spectral window from 4000 to 600 cm^{-1} . Abbreviations used for chemicals: NMP, *N*-methyl-2-pyrrolidone; DMAc, dimethylacetamide; DMF, dimethylformamide; COD, 1,5-cyclooctadiene; bipy, 2,2'-bipyridine; Et_2O, diethyl ether; DCM, dichloromethane; MeCN, acetonitrile; EtOAc, ethyl acetate; EtOH, ethanol.

2. Materials and Methods

2.1 **Materials**

All commercial reagents were used as received unless stated otherwise. $Ni(MeCN)_2Br_2$ was synthesized by collecting the solids from the receiving flask of MeCN soxhlet extraction of anhydrous $NiBr_2$ under an inert atmosphere. $Ni(COD)_2$ was purchased from Strem. $NiBr_2$ was purchased from Alfa Aesar or Strem, all $NiBr_2$ used was anhydrous. 1,5-cyclooctadiene (COD, freeze-pump-thawed and stored in Schlenk tube in N_2 atmosphere glovebox), and zinc dust (activated according to literature[1]) were purchased from Sigma-Aldrich. N,N-dimethylformamide (99.8%, Extra Dry over Molecular Sieve, AcroSeal™) was purchased from Fisher and was freeze-pump-thawed and stored over 3 Å molecular sieves before use. 2,2'-bipyridine (bipy) was purchased from Chem-impex and Ambeed. Br_2 was purchased from Sigma-Aldrich. Ethanol (200 proof, anhydrous) was purchased from Decon Labs. Sodium metabisulfite was purchased from Fisher. 1,3,5-(4-bromophenyl)benzene was purchased from Ambeed. It was purified by washing the solid with MeOH to remove residual 4-bromophenylacetylene. 2,2',7,7'-tetrabromo-9,9'-spirobifluorene was purchased from Ambeed. *n*-butyl lithium (2.5 M in hexanes) was purchased from Fisher. Ethyl acetate (HPLC grade) was purchased from Fisher. Hexanes (ACS grade) was purchased from Fisher. Diethyl carbonate was purchased from Acros. Diethyl ether (99+%, BHT inhibited) was purchased from Acros. 1,4-bis(triethoxysilyl)benzene was purchased from Ambeed. Methanol (ACS grade) was purchased from Fisher. Dichloromethane (ACS grade) was purchased from Millipore. Chloroform (ACS grade) was purchased from Millipore. Tetrahydrofuran (ACS grade, BHT inhibited) was purchased from Sigma-Aldrich. 1,4-dibromobenzene was purchased from Sigma-Aldrich. Silicon tetrachloride was purchased from Sigma-Aldrich. Sulfuric acid (concentrated) was purchased from Sigma-Aldrich. Isoamyl nitrite was purchased from Sigma-Aldrich. Hypophosphorous acid (50% in water) was purchased from Sigma-Aldrich. Aniline was purchased from Thermo Scientific and was stored at 4 °C. Trityl chloride was purchased from Acros. Potassium carbonate was purchased from Fisher. NMP (anhydrous, freeze-pump-thawed and stored over sieves in N_2 atmosphere glovebox) was purchased from Sigma-Aldrich. DMAc (anhydrous, freeze-pump-thawed and stored over sieves in N_2 atmosphere glovebox) was purchased from Sigma-Aldrich. Molecular sieves (3 Å) were purchased from Acros and were activated for 36 hours at 210 °C in a vacuum oven (~0.5 torr).

2.2 Gas Adsorption Isotherms

Gas adsorption isotherms were determined by a volumetric method using a Micromeritics 3Flex instrument. Samples (35-60 mg) were first desolvated 80 °C for 12 hours under vacuum at ~0.1 torr to remove bulk solvent and other volatile contaminants. The activated samples were then transferred to a pre-weighed glass analysis tube capped with either a micromeritics TranSeal or CheckSeal. The samples were further activated for 2-18 hours on a Micromeritics **VacPrep 061** at 180 °C (~$3x10^{-2}$ mmHg). Free space measurements were performed using ultra high purity He. Nitrogen adsorption isotherms (**Figs. S4 to S26**) were obtained using ultra-high purity nitrogen and a 77 K liquid-N_2 bath. Carbon dioxide isotherms were measured using 99.99% purity CO_2 in a 273 K water/ethylene glycol bath maintained with a micromeritics ISO controller.

Pore size calculations here using the micromeritics microactive software NLDFT model of slit pores of N_2 on carbon (slits) at 77 K. We note that pore size analysis of amorphous microporous materials is fraught with challenges, the main purpose of these is not to determine *absolute* pore size distribution, but to show *relative* pore size distributions relative to conventional $Ni(COD)_2$ based methods.

2.3 Thermogravimetric Analysis (TGA)

Thermogravimetric analysis was conducted using an SDT Q600 TGA–DTA analyzer (TA Instruments). ~3–5 mg of sample was heated at 35 °C for 30 min under flowing oxygen (100 mL min^{-1}), ramped to 750 °C at a rate of 10 °C min^{-1}, and then was isothermal for 10 min at 750 °C.

2.4 Powder X-Ray Diffraction (PXRD)

A Bruker Phaser II model X-ray diffractometer equipped with a Cu anode was employed to acquire diffraction patterns in the range 2Θ = 8 - 60°. Samples were loaded onto a zero-background quartz sample holder for all measurements.

2.5 Scanning Electron Microscopy (SEM)

SEM images of samples deposited on carbon-coated adhesive tape were obtained using a JEOL JSM-7600F field emission scanning electron microscope operated at an accelerating voltage of 5 kV in high-vacuum mode. The samples on adhesive tape were gold-sputtered prior to the analysis at 200 mTorr for 30 s at an out-put range of 50-100 mA.

2.6 Fourier Transform Infrared Spectra (FTIR)

FTIR specra were collected on an Cary 620 FTIR spectrometer equipped with a diamond anvil sampling module. Spectra were collected from 600 cm^{-1} to 4000 cm^{-1} with 4 cm^{-1} resolution.

2.7 Solid-State Nuclear Magnetic Spectroscopy (ssNMR)

Solid-state NMR spectra were not collected on the PAFs described herein for the following reasons: (1) local structure of PAFs is generally inferred from the monomer structure and polymerization mechanism. More detailed structural considerations (e.g. dangling end defectivity) or extended topological defectivity are beyond the scope of this study. (2) The primarily aromatic composition of the PAFs described in this paper are supported by elemental analysis, FTIR spectra, and their synthesis. The presence of non-aromatic motifs in **P-5** and **P-7** are corroborated by the FTIR spectra. (3) The structural information provided by such spectra is unlikely to provide important insights into surface area or total porosity, the focus of these studies.

3. Monomer Synthesis

3.1 Tetrakis(4-bromophenyl)methane

Pre-reaction notes:

1. We have found that the synthesis of high surface area **P-1** (PAF 1), and likely other PAFS, is critically dependent on Tetrakis(4-bromophenyl)methane (**M-1**) purity. Many of the impurities encountered in our optimization of this synthesis exhibit comparable ^{1}H NMR spectra and silica TLC retention factors to **M-1**. We recommend additional characterization of purity through other methods such as LC/MS or HPLC and careful attention to overlapping peaks in high field ^{1}H NMR.
2. Many of these impurities seem to be introduced during the diazotization/reduction sequence in the synthesis of tetraphenylmethane. These impurities were minimized through careful adherence to the procedure below. Should purity issues persist, we recommend additional purification through one of the three following methods:
    a. Purification of tetraphenylmethane through sublimation at 195 °C at 5x10 $^{-3}$ mmHg,[15] or
    b. Purification of Tetrakis(4-bromophenyl)methane silica column chromatography (100% hexane)[2] or
    c. Purification of Tetrakis(4-bromophenyl)methane by recrystallization through the following procedure: Dissolve the crude tetrakis-(4-bromophenylmethane) in $CHCl_3$ as a 0.11 M solution. Filter this solution through Fisherbrand Q5 filter paper. Next, charge a pressure equalized liquid addition funnel with 1 volume equivalent of EtOH relative to the $CHCl_3$ used to make the 0.11 M solution. Add the EtOH dropwise over 1 hour to the stirring $CHCl_3$ solution of tetrakis(4-bromophenylmethane). Let stand overnight at ~4 °C. Collect the white powder on a glass frit and dry under vacuum. Crystallization yields ~60% from crude mass were obtained through this method.

Tetrakis(4-bromophenyl)methane was synthesized in three steps from (chloromethanetriyl)tribenzene.

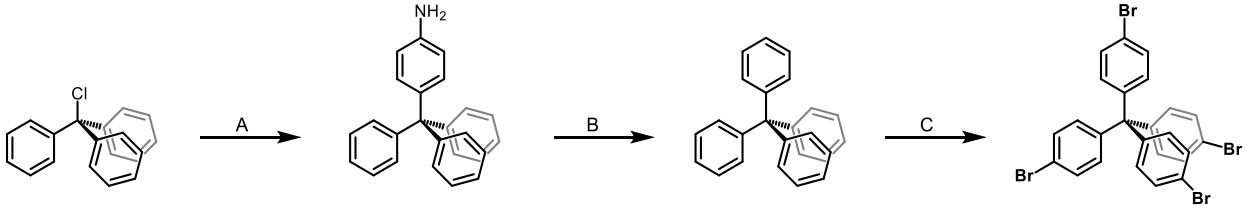

3.1.1 4-Tritylaniline

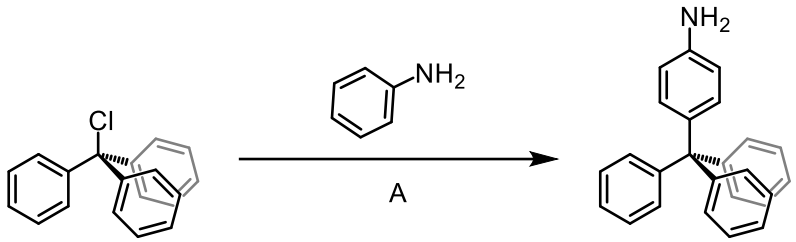

(**A**) 4-trityl aniline was synthesized via a modified literature procedure.[3] A 250 mL round bottom flask was equipped with a stir bar and charged with trityl chloride (12.0 g, 43.15 mmol, 1 eq) and aniline (30 mL, 328 mmol, 7.60 eq). The reaction flask was moved onto a Schlenk line and vac-refilled three times. The vessel was then heated to 215 °C under N_2 for 5 min, and then 20 min without N_2. Once cooled to room temperature, HCl (2 M, 30 mL) and MeOH (30 mL) were added to the flask, and it was brought to reflux for 10 min. Once cooled to room temperature, the reaction was filtered with a fritted funnel to obtain a purple solid. This solid was washed with copious water and let dry under air over night. The next day this solid was fully converted to the free base by stirring over a N_2 sparged mixture of K_2CO_3 (14.85 g, 108 mmol) in EtOH (200 mL) overnight. The reaction was vacuum filtered, washed with water (240 mL), and dried under vacuum to give the free-base 4-trityl aniline as a purple solid (13.2 g, 39.4 mmol, 91% yield). NMR spectra were consistent with literature reports.[4]

^{1}H NMR (400 MHz, $(CD_3)_2SO$, 23 °C): δ 7.29-7.05 (multiple peaks, 15H), 6.72 (d, J = 8 Hz, 2H), 6.44 (d, J = 8 Hz, 2H), 4.97 (s, 2H).

3.1.2 Tetraphenylmethane

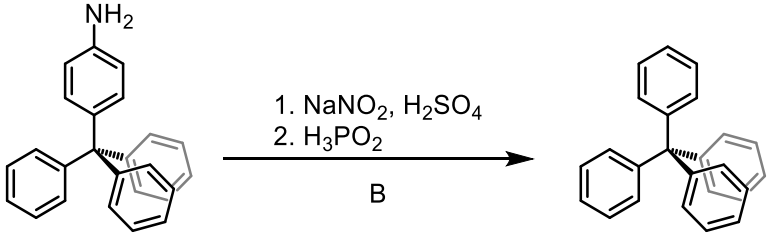

(**B**) Tetraphenylmethane was synthesized according to literature procedure.[5] Reaction vessel was equipped with a stir bar and charged with EtOH (190 mL), concentrated H_2SO_4 (27 mL), and 4-trityl aniline (13.2 g, 39.4 mmol). It was then cooled to -10 °C in an ice/acetone bath. Once cooled, isoamyl nitrite (24 mL, 178.6 mmol) was added dropwise from an addition funnel and the reaction stirred for 30 min. Next, 50% hypophosphorous acid (43 mL, 485 mmol) was added dropwise from the addition funnel. After the addition, the flask was stirred for 5 minutes then heated to 50 °C for 2 hours. The reaction was filtered, washed with DMF, H_2O, and EtOH, and air dried to yield Tetraphenylmethane as a tan solid (11.84 g, 37 mmol, 94% yield). NMR spectra were consistent with literature reports.[5]

^{1}H NMR (400 MHz, $(CD_3)_2SO$, 23 °C): δ 7.35-7.05 (multiple peaks, 20H). Note: tetraphenylmethane has limited solubility in $(CD_3)_2SO$. This solvent was used because it resolved impurity peaks better than $CDCl_3$. Care was taken to ensure all solids dissolved.

3.1.3 Synthesis of tetrakis(4-bromophenyl)methane (M-1)

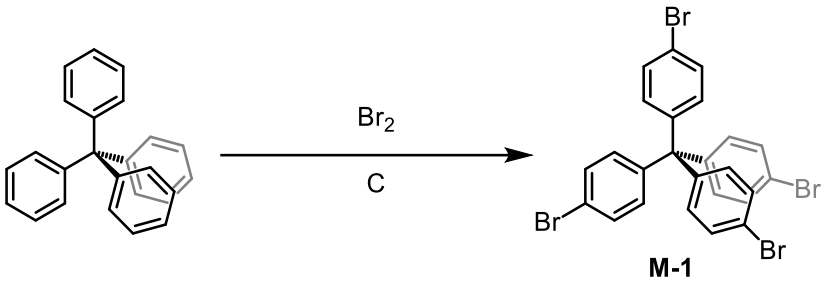

(**C**) Tetrakis(4-bromophenyl)methane was synthesized via a modified literature procedure.[6] A 500 mL round bottom flask was equipped with a stir bar, addition funnel, N_2 inlet, and outlet leading to a NaOH quenching solution. An empty flask was placed between the outlet and the reaction flask according to the scheme below (**Figure S1**).

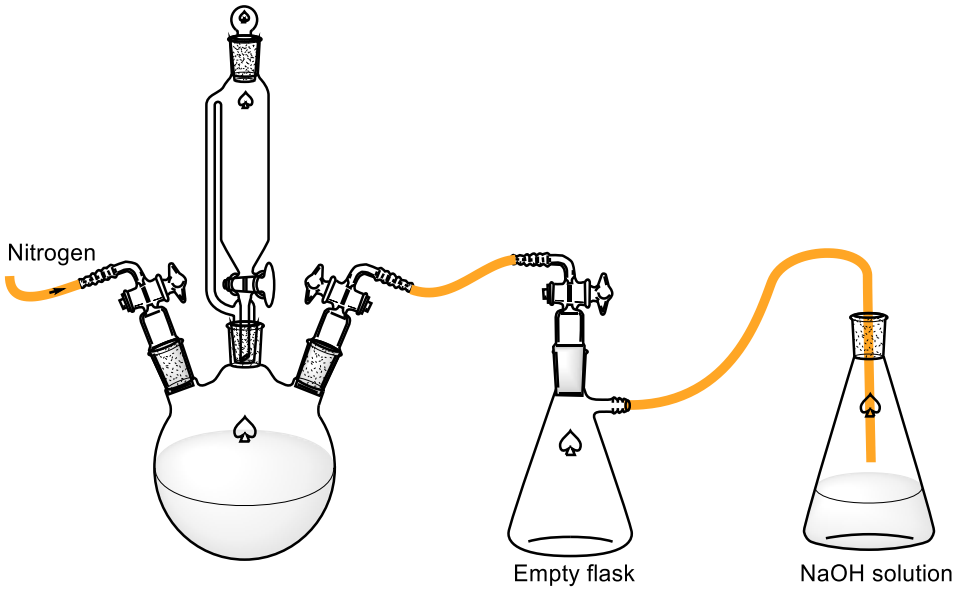

Figure S1. Reaction apparatus for bromination of tetraphenylmethane.

The reaction vessel was then charged with tetraphenylmethane (10 g, 31.2 mmol). Bromine (17.8 mL, 343 mmol) was added dropwise from the addition funnel. The resulting slurry was stirred at room temperature for 20 min before being cooled to -78 °C in a dry ice/acetone bath. Once cooled, EtOH (200 mL) was slowly added. The inlet, outlet, and addition funnel were then removed and replaced with rubber septa that were secured with electrical tape and parafilm. The reaction mixture was sonicated for 20 min to break up the large chunks. After sonication, the reaction was left to stir overnight at room temperature. The reaction was then subjected to vacuum filtration with a M fritted funnel. The filter cake was washed with DI H_2O (100 mL), sat. aqueous sodium metabisultife (100 mL), followed by DI H_2O (100 mL). The off-white filter cake was air-dried for two days, followed by drying on vacuum line. The product was purified by recrystallization in accordance to the pre-reaction notes to yield tetrakis(4-bromophenyl)methane as a light tan solid (7.25 g, 11.4 mmol, 37% yield). NMR spectra were consistent with literature reports.[5]

^{1}H NMR (400 MHz, CD_3Cl, 23 °C): δ 7.39 (d, J = 8 Hz, 8H), 7.01 (d, J = 12 Hz, 8H).

3.2 Synthesis of tetrakis(4-bromophenyl)silane (**M-2**)

Tetrakis(4-bromophenyl)silane was synthesized in one step from $SiCl_4$ using a modified literature procedure.[7]

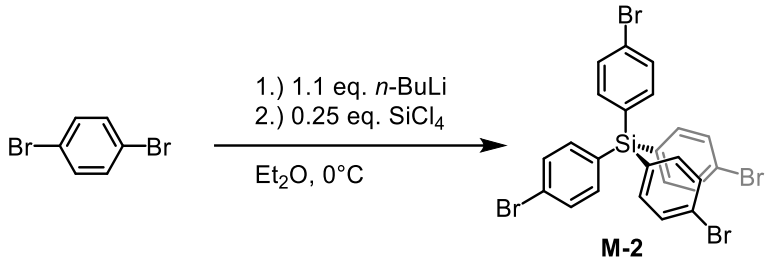

M-2

A 500 mL Schlenk tube was flame dried and moved into a N_2 atmosphere glovebox. After cooling to room temperature, it was then charged with 1,4-dibromobenzene (8.35 g, 35.4 mmol) and Et_2O (250 mL, anhydrous, over sieves). The flask was capped and removed from the glovebox and moved onto a Schlenk line. The reaction was put under N_2 and cooled to 0 °C in an ice bath. Once cooled, *n*-BuLi (2.5 M in hexanes, 14.2 mL, 35.4 mmol) was added dropwise and the reaction stirred for 30 min. Then, $SiCl_4$ (1.02 mL, 8.85 mmol) was added dropwise with a syringe and the reaction was stirred for 20 hours. The reaction was quenched with DI water (100 mL), DCM (200 mL) was added, and the organic layer separated. The aqueous layer was then washed with DCM (100 mL, x3), all organic fractions combined, dried with $MgSO_4$, and concentrated to dryness under vacuum. The crude was recrystallized from EtOAc to give white crystals (2.21 g, 3.4 mmol, 38% yield). NMR spectra were consistent with literature reports.[8]

^{1}H NMR (400 MHz, $CDCl_3$, 23 °C): δ 7.54 (d, J = 8 Hz, 8H), 7.34 (d, J = 8 Hz, 8H).

3.3 Synthesis of tris(4-bromophenyl)methanol (**M-5**)

Tris(4-bromophenyl)methanol was synthesized in one step from p-dibromobenzene using a modified literature procedure.[5]

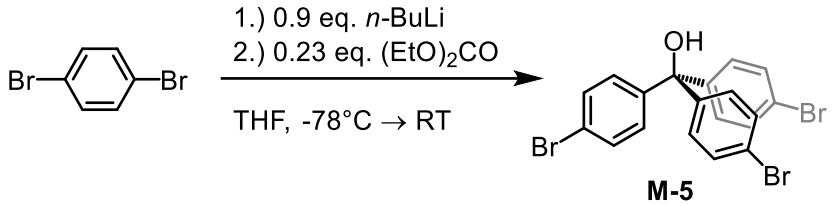

M-5

A 200 mL Schlenk flask was oven dried and moved into a N_2 glovebox. After cooling to room temperature, it was then charged with 1,4-dibromobenzene (4.35 g, 18.4 mmol). The flask was removed from the glovebox, put under N_2, and submerged into a dry ice bath/acetone bath at -78 °C. Once cooled, *n*-BuLi (2.5 M in hexanes, 7 mL, 17.5 mmol) was added dropwise with a syringe. The reaction was held at -78 °C for 2.5 hours. Diethyl carbonate (0.51 mL, 4.2 mmol) was then added to the reaction via syringe and the reaction was removed from the dry ice bath. The reaction was stirred 18 hours at room temperature. It was then quenched with saturated aqueous ammonium chloride (25 mL). The reaction was transferred to a separatory funnel and extracted with EtOAc (25 mL, x2). The combined organic layers were washed with brine and concentrated under vacuum. The obtained yellow oil was suspended in MeOH (15 mL) and put under -25 °C for 10 days. The crystals were collected by vacuum filtration with a fritted funnel and tris(4-bromophenyl)methanol was obtained as a white solid (1.6 g, 3.2 mmol, 52% yield). NMR spectra were consistent with literature reports.[5]

^{1}H NMR (400 MHz, $CDCl_3$, 23 °C): δ 7.45 (d, J = 8 Hz, 6H), 7.12 (d, J = 8 Hz, 6H). Note the OH hydrogen was not observed via ^{1}H NMR

3.4 Synthesis of 1,4-bis(tris(4-bromophenyl)silyl)benzene (**M-6**)

1,4-bis(tris(4-bromophenyl)silyl)benzene was synthesized in one step from 1,4-bis(triethoxysilyl)benzene via a modified literature procedure.[9]

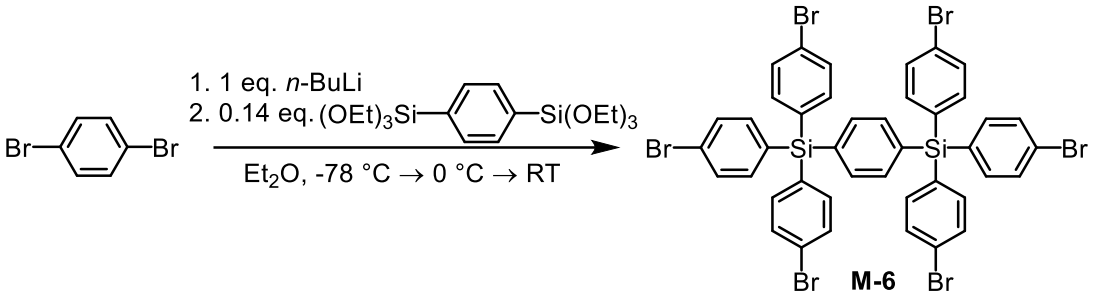

A 100 mL Schlenk flask was moved into a N_2 atmosphere glovebox and loaded with 1,4-dibromobenzene (4.15 g, 17.6 mmol) and Et_2O (15 mL). An addition funnel was attached to the flask and sealed with a septum. The flask was then moved out of the glovebox, moved onto a Schlenk line, and then cooled to -78 °C in a dry ice/acetone bath. *n*-BuLi (2.5 M in hexanes, 7 mL, 17.5 mmol) diluted in Et_2O (10 mL) was injected into the addition funnel and added into the flask dropwise. The reaction mixture was stirred at –78 °C for 1 hour and warmed to 0 °C. 1,4-bis(trisethoxysilyl)benzene (1 mL, 2.53 mmol) was dissolved in Et_2O (3 mL) and added dropwise by addition funnel. The reaction mixture was stirred at room temperature overnight. Then the reaction was quenched by DI H_2O (5 mL) and the organic layer was separated, washed with brine, and dried with $MgSO_4$. The resulting solution was put inside the freezer overnight to precipitate the crude product. Recrystallization was then performed from EtOAc to give the final product 1,4-bis(tris(4-bromophenyl)silyl)benzene (320 mg, 0.30 mmol, 10% yield). NMR spectra were consistent with literature reports.[9]

^{1}H NMR (400 MHz, $CDCl_3$, 23 °C): δ 7.59-7.49 (multiple peaks, 16H), 7.35 (d, J = 8 Hz, 12H).

3.5 Synthesis of tetrakis(4-bromophenyl)adamantane (**M-7**)

Tetrakis(4-bromophenyl)adamantane was synthesized in one step from 1,3,5,7-tetraphenyladamantane via a modified literature procedure.[10]

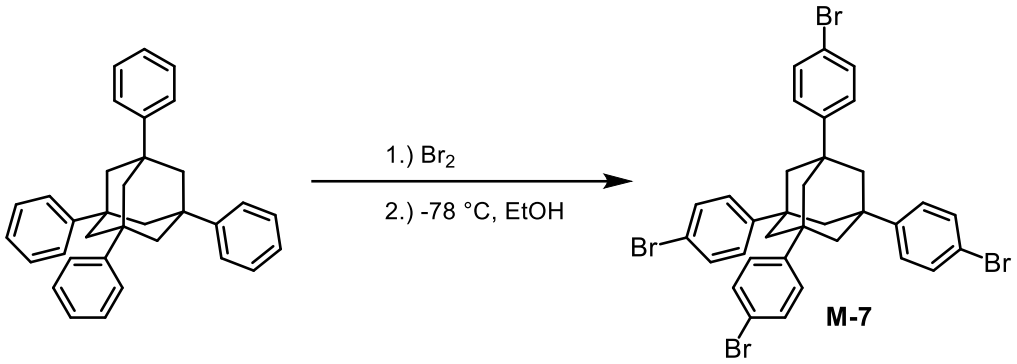

A 100 mL round-bottom flask was equipped with a stir bar, and addition funnel. The reaction vessel was charged with 1,3,5,7-tetraphenyladamantane (500 mg, 1.14 mmol), followed by the dropwise addition of bromine (0.6 mL, 11.6 mmol), and stirred for 20 min. It was then cooled to -78 °C in a dry ice/acetone bath, EtOH (50 mL) was added, and the reaction stirred overnight. The reaction was filtered with a M fritted funnel, washed with sat. sodium metabisulfite (60 mL), and DI H_2O (60 mL x 2). The filter residue was transferred to a 100 mL recovery flask, suspended in MeOH (50 mL), and heated at 40 °C for 1 hour. After cooling to room temperature, the reaction was gravity filtered and concentrated to dryness under vacuum. The product was purified by recrystallization from $CHCl_3$ to yield tetrakis(4-bromophenyl)adamantane as white crystals (524 mg, 0.69 mmol, 60.8% yield). NMR spectra were consistent with literature reports.[10]

^{1}H NMR (400 MHz, $CDCl_3$, 23 °C): δ 7.47 (d, J = 8 Hz, 8H), 7.32 (d, J = 8 Hz, 8H), 2.07 (s, 12H).

4 Optimization of PAF-1 (P-1) Synthesis

Pre reaction notes:

1. Solvents must be strictly deoxygenated. The solvent used in all reactions was deoxygenated through at least three thorough freeze-pump-thaw cycles.
2. Zn dust activation was performed to provide consistency to the reduction of Ni(II) to Ni(0) between Zn dust batches or suppliers. Preliminary experimentation suggests that non-activated Zn dust used directly after purchase from the manufacturer can also be effective, but variable. However, the reduction of the green Ni(II) to the characteristic purple color of Ni(0)(bipy) complexes was notably slower with unactivated Zn dust. In an effort to minimize sources of variability from extent of Zn dust passivation, we strongly recommend Zn dust activation through the following procedure below. We found it yielded consistent Zn from batch to batch.

Zinc Dust Activation:

Zinc dust was activated by a modified literature procedure.[1] Under a N_2 atmosphere, a 100 mL round-bottom flask was charged with Zn dust (5.00 g, 76.9 mmol), followed by the dropwise addition of trimethylchlorosilane (0.725 mL, 5.7 mmol). The mixture was stirred at room temperature for 50 min before vacuum filtration with a fine fritted glass funnel. Alternatively, the filtration step can be done under air if the activated Zn dust will be used or stored under N_2 quickly. We found activated Zn dust filtered under air used within an hour of filtration to be equivalent to Zn dust that was activated, filtered, and stored under N_2.

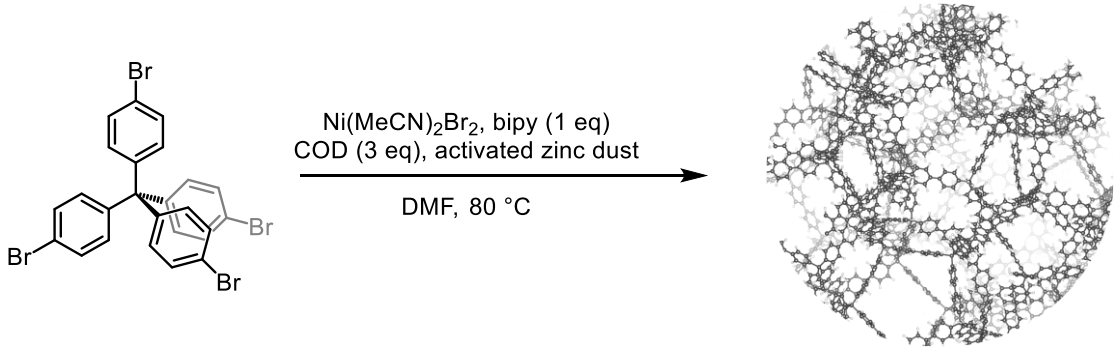

M-1 **P-1**

Synthesis of P-1. A modified literature procedure was followed.[11] Inside a N_2 atmosphere glovebox, a 20 mL scintillation vial was loaded with anhydrous DMF (10 mL), $Ni(MeCN)_2Br_2$ (0.82 mmol), COD (264 mg, 2.5 mmol), bipy (256 mg, 1.64 mmol), and activated zinc dust (67 mg, 1.03 mmol), in that order. The mixture was stirred at 25 °C for 5 hours. The reaction was then heated at 80 °C for 5 min, followed by the portion wise addition of tetrakis(4-bromophenyl)methane (110 mg, 0.17 mmol). The reaction was stirred at 80 °C for 23 hours, removed from the glovebox, opened to air, transferred to a 50 mL round-bottom flask with DMF (10 mL), and cooled to room temperature. Once cooled, the reaction was quenched with the dropwise addition of 6.0 M HCl (10 mL). The reaction was stirred open to air for 20 hours, followed by vacuum filtration with a medium porosity fritted funnel. The filter cake was then washed with 20 mL each of: DMF, MeOH, $CHCl_3$, CH_2Cl_2, and THF. The product was dried in vacuo to produce **P-1** as a white powder. Yields ranged from 65% to 80% based on theoretical structure.

Note: $Ni(MeCN)_2Br_2$ was used initially to minimize complications due to insolubility of conventional nickel salts. Later iterations of these reactions, and the focus of the manuscript, utilized commercially available NiX_2 salts.

Table S1. Table of conditions optimized during the synthesis of PAF-1.

Entry	Change from Standard	SA_{BET} (m^2g^{-1})
1	none	3482[a]
2	0.5 eq bipy	3308
3	1.25 eq bipy	4181
4	3 eq bipy	5058
5	$NiCl_2$ instead of $NiBr_2(MeCN)_2$, 2 eq bipy	2447
6	$Ni(OAc)_2$ instead of $NiBr_2(MeCN)_2$, 2 eq bipy	Not isolated
7	Magnesium instead of activated Zn dust	1374
8	Manganese instead of activated Zn dust	Not isolated
9	Magnesium instead of activated Zn dust, 2 eq bipy	3076
10	Manganese instead of activated Zn dust, 2 eq bipy	2759
11	TDAE[b] instead of activated Zn dust, 2eq bipy	Not isolated
12	NMP instead of DMF, 2 eq bipy	3198
13	DMAc instead of DMF, 2 eq bipy	4618
14	$NiBr_2$, 2 eq bipy, 1 hr 80 °C pre-stir	4940[c]

[a]Average of five polymerizations. [b]TDAE = tetrakis(dimethylamino)ethylene [c]Average of two polymerizations

5 Polymer Scope

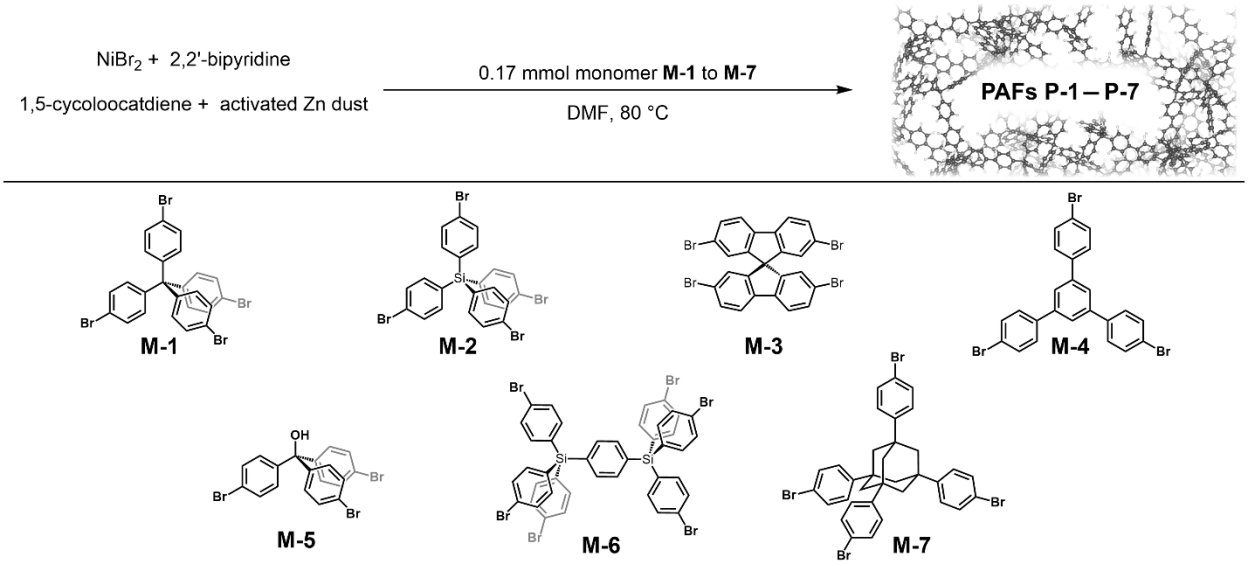

Pre-reaction Note: Because monomers with four C-Br bonds will need more nickel mediator than monomers with three C-Br bonds, the stoichiometry of all reagents except the monomer was held constant relative to the mmol of C-Br, not mmol of monomer. For example, in a standard reaction 1.2 equivalents of Ni is used per C-Br bond. The standard reaction of 0.17 mmol of **M-1** (4 C-Br bonds, 0.68 mmol of C-Br) would require 0.82 mmol of $NiBr_2$ (0.68 mmol C-Br x 1.21 Ni/C-Br= 0.82 mmol of Ni).

General PAF synthesis (Method A). Inside an inert atmosphere glovebox**,** a 20 mL scintillation vial was loaded with anhydrous DMF (10 mL), $NiBr_2$ (1.2 mmol per mmol of C-Br), COD (3.6 mmol 3 eq relative to Ni), and bipy (2 eq relative to Ni). The reaction was heated at 80 °C for 1 hour. Next, the activated zinc (1.5 mmol per mmol of C-Br) was added, heated for 5 min, followed by the portion wise addition of monomer (0.17 mmol) over 2 min. The reaction was stirred at 80 °C for 20-23 hours, removed from the glovebox, opened to air, diluted with DMF (10 mL), and cooled to room temperature. Once cooled, it was quenched with the dropwise addition of 6.0 M HCl (10 mL/0.17 mmol monomer). The reaction was stirred open to air for 19-22 hours, followed by vacuum filtration with a medium porosity fritted funnel. The filter cake was then washed with 30 mL each of: DMF, MeOH, $CHCl_3$, CH_2Cl_2, and THF in that order.[11] The product was dried at 80 °C under vacuum (~0.1 torr) to produce the corresponding PAF. Yields were between 66% and 85% based on the theoretical structure. Percent yields were calculated based on the amount of sample in the isotherm sample tubes. We expect actual yields to be higher due to losses in transfers between containers.

Representative Synthesis of PAF-1 (P-1) via Method A. Inside an inert atmosphere glovebox, a 20 mL scintillation vial was loaded with anhydrous DMF (10 mL), $NiBr_2$ (179 mg, 0.82 mmol), COD (264 mg, 2.5 mmol), and bipy (256 mg, 1.64 mmol). The reaction was heated at 80 ºC for 1 hour. Next, the activated zinc (67 mg, 1.03 mmol) was added, heated for 5 min, followed by the portion wise addition of tetrakis(4-bromophenyl)methane (**M-1**) (110 mg, 0.17 mmol) over 2 min. The reaction was stirred at 80 ºC for 22 hours, removed form the glovebox, opened to air, diluted with DMF (10 mL), and cooled to room temperature. Once cooled, it was quenched with the dropwise addition of 6.0 M HCl (10 mL). The reaction was stirred open to air for 20 hours, followed by vacuum filtration with a medium porosity fritted funnel. The filter cake was then washed with 30 mL each of: DMF, MeOH, $CHCl_3$, CH_2Cl_2, and THF in that order. The product was dried at 80 ºC under vacuum (~0.1 torr) to produce **P-1** (45 mg, 84% yield based on theoretical structure). Samples used for porosimetry were further activated as described in section 2.2.

$Ni(COD)_2$ PAF synthesis (Method B).

The Zn based method was benchmarked against a standardized $Ni(COD)_2$ procedure. This procedure is listed below.

Procedure based on literature.[11] Inside an inert atmosphere glovebox, a 20 mL scintillation vial was loaded with anhydrous DMF (10 mL), bipy (1.17 mmol, 1 eq relative to $Ni(COD)_2$), COD (1.17 mmol, 1 eq relative to $Ni(COD)_2$), and $Ni(COD)_2$ (1.17 mmol, 1.21 mmol/C-Br). The mixture was stirred at room temperature for 1.5-2 hours, then moved to a pre-heated 80 °C hot plate and stirred for 20 min. Monomer (0.24 mmol) was added portion wise over 2 min and the reaction stirred at 80 °C for 22 hours. It was then removed from the glovebox, opened to air, diluted with DMF (10 mL), and cooled to room temperature. Once cooled, it was quenched with the dropwise addition of 6.0 M HCl (10 mL/0.24 mmol monomer) and stirred open to air for 20 hours. The polymer was isolated via vacuum filtration with a medium porosity fritted funnel, and washed with 30 mL each of: DMF, MeOH, $CHCl_3$, CH_2Cl_2, and THF. The resulting solid was dried at 80 °C under vacuum (~0.1 torr) to yield the PAF. Yields were between 46% and 98% based on the theoretical structure. Percent yields were calculated based on the amount of sample in the isotherm sample tubes. We expect actual yields to be higher due to losses in transfers between containers.

Table S2. Surface area for PAFs made by methods A and B.

Material	Reference Name	Method	SA_{BET} (m^2 g^{-1})	V_{tot} (cm^3 g^{-1})[a]	Percent Yield[b]
P-1	PAF-1[11]	A	4940[c]	2.50	69%
		B	4651	2.34	98%
P-2	PAF-3[12]	A	4773	2.63	66%
		B	4225	2.37	70%
P-3	PS1-C[13]	A	1595	1.43	76%
		B	2237	1.76	58%
P-4	PAF-5[14]	A	2042	1.93	78%
		B	2313	1.58	70%
P-5	TAF-OH[15]	A	1386	0.77	85%
		B	1423	0.81	67%
P-6	PAF-100[16]	A	3968	2.16	78%
		B	3947	2.06	75%
P-7	PPN-3[17]	A	2440	1.60	46%
		B	2340	1.51	60%

[a] Total pore volume based on single point pore volume at p/p_0 =0.95 [b] Yield based on theoretical structure. [c] Average of two polymerizations.

6 Schlenk Line Synthesis of P-1 (Method C)

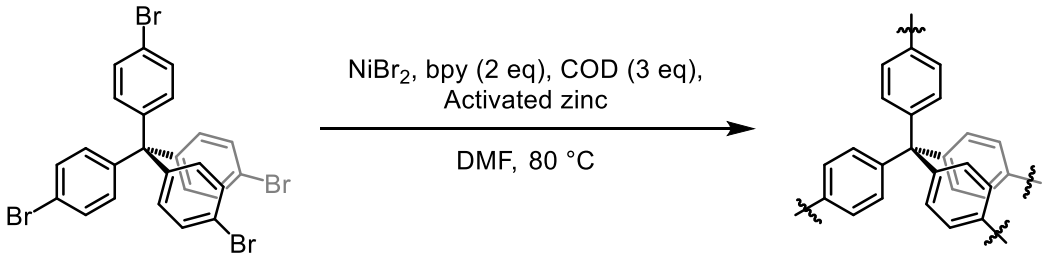

M-1 **P-1**

Zinc dust was used quickly (within an hour) after it was activated via treatment of the Zn dust with TMSCl in dry THF and filtered under air. (See section 4 for more details)

Small Scale

An oven dried 250 mL 3-neck round bottom flask was equipped with two oven dried solid addition funnels and an oven dried Claisen adapter. The solid addition funnel for the monomer was equipped with a stir bar and a magnet was electrical taped to the outside (**Figure S2-A**). The top

port of the Claisen adapter was fitted with a septum and the side was fitted with a hose barb adapter. All joints were greased, secured with Keck clips, and the reaction vessel was cooled under vacuum. Once cooled, the vessel was backfilled with N_2.

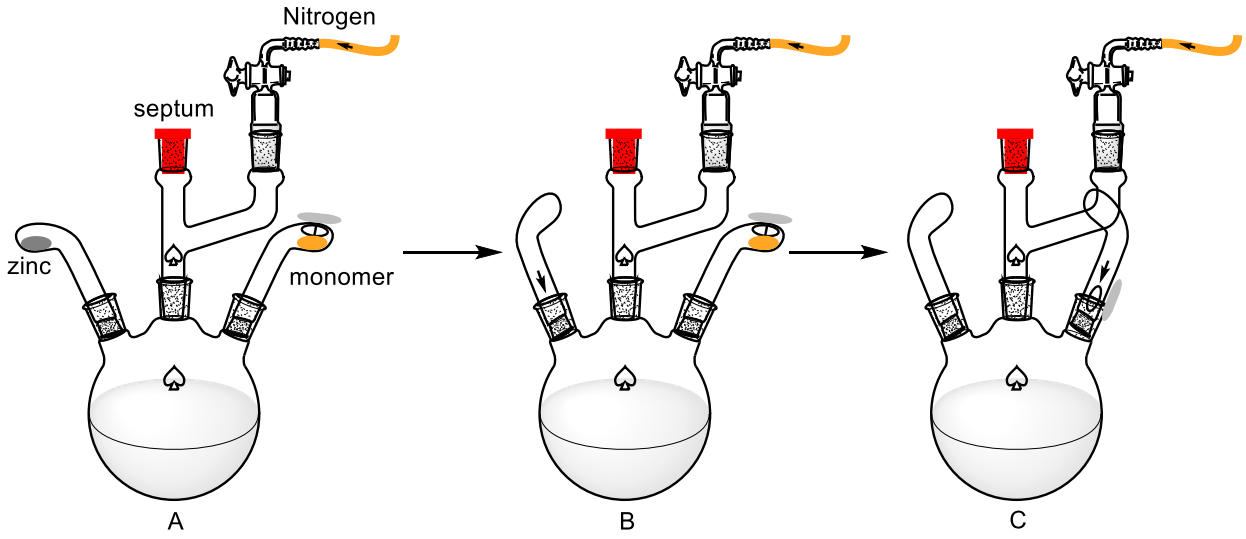

Figure S2: (A) Reaction setup for Schlenk line synthesis. Left addition funnel filled with zinc, right filled with monomer with magnet electrical taped to outside. **(B)** Addition funnel turned to add zinc. Stirred for 5 min at 80 °C. **(C)** Addition funnel turned to add monomer. Stir bar was manipulated with magnet to facilitate its addition and break up clogs.

One solid addition funnel was filled with activated zinc dust (466 mg, 7.14 mmol, left addition funnel **Figure S2-A**) and the other filled with tetrakis(4-bromophenyl)methane (0.750 g, 1.18 mmol, right addition funnel **Figure S2-A**). The vessel was loaded with $NiBr_2$ (1.25 g, 5.72 mmol), bipy (1.78 g, 11.39 mmol), and vac refilled three times. DMF was then added via cannula (60 mL), followed by the addition of deoxygenated COD (2.13 mL, 17.36 mmol, via syringe). The reaction was then heated to 80 °C for 1 hour, followed by the addition of the zinc via the solid addition funnel. After stirring for 5 min, the monomer was added via the other solid addition funnel. The reaction stirred for 22 hours at 80 °C. It was then cooled to room temperature, opened to air, and quenched with 6 M HCl (70 mL). The reaction quenched for 19 hours open to air, and the polymer collected via vacuum filtration with a M fritted funnel. The filter residue was washed with 100 mL each of DMF, MeOH, CH_2Cl_2, $CHCl_3$, and THF.[11] It was then dried under vacuum at 80 °C and the polymer was obtained as a white solid (298 mg, 80% yield based on theoretical structure). The BET surface area of polymer obtained through this procedure was 4721 $m^2 g^{-1}$ as determined from N_2 isotherms at 77 K.

Large Scale

On the bench, an oven dried 500 mL 3-neck round bottom flask was equipped with two oven dried solid addition funnels and an oven dried Claisen adapter. The solid addition funnel for the monomer was equipped with a stir bar and a magnet which was electrical taped to the outside (**Figure S2-A**). The top port of the Claisen adapter was fitted with a septum and the side was fitted with a hose barb adapter. All joints were greased and clipped and the reaction vessel was cooled under vacuum. Once cooled, the vessel was backfilled with N_2.

One solid addition funnel was filled with activated zinc dust (1.68 g, 25.7 mmol) and the other filled with tetrakis(4-bromophenyl)methane (2.7 g, 4.25 mmol). The vessel was loaded with $NiBr_2$ (4.49 g, 20.55 mmol), bipy (6.42 g, 41.14 mmol), and evacuated and refilled three times. DMF was then added via cannula (180 mL), followed by the addition of COD (7.7 mL, 62.53 mmol, via syringe). The reaction was then heated to 80 °C for 1 hour, followed by the addition of the activated zinc dust via the solid addition funnel. After stirring for exactly 5 min, the monomer was added via the other solid addition funnel. The stirbar inside the funnel was manipulated using the magnet on the outside of the funnel to break up any clumps precluding smooth addition of the solid. The reaction stirred for 22 hours at 80 °C. It was then cooled to room temperature, dumped into a 500 mL beaker under air, and quenched with 6 M HCl (100 mL). The quench stirred for 19 hours open to air, and the polymer was collected via vacuum filtration with a M fritted funnel. The filter residue was washed with 100 mL each of DMF, MeOH, CH_2Cl_2, $CHCl_3$, and THF. It was then dried under vacuum at 80 °C and the polymer was obtained as a white solid (1.21 g, 90% yield based on theoretical structure). The BET surface area of polymer obtained through this procedure was 4450 $m^2 g^{-1}$ as determined from N_2 isotherms at 77 K.

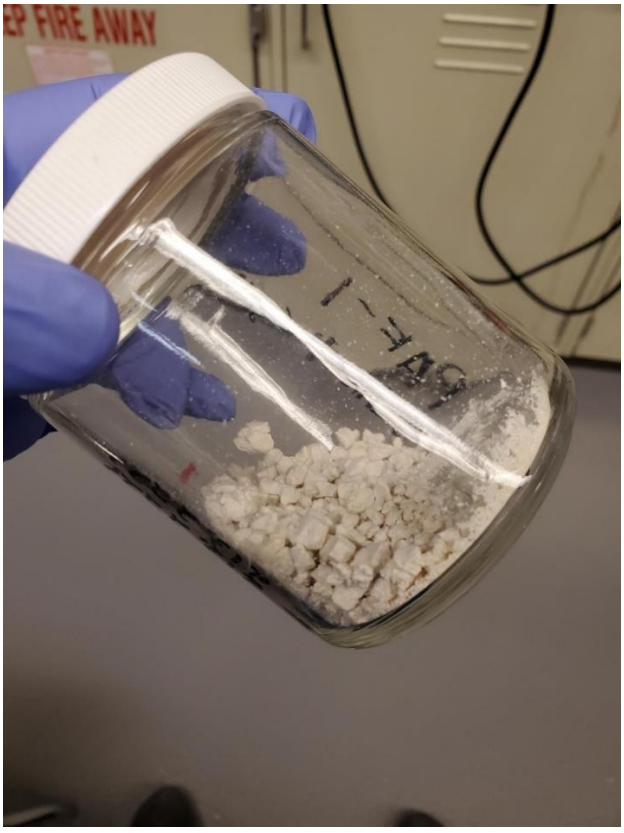

Figure S3: Isolated **P-1** from large scale Schlenk synthesis.

7 Characterization Data

7.1 N_2 Isotherms at 77 K

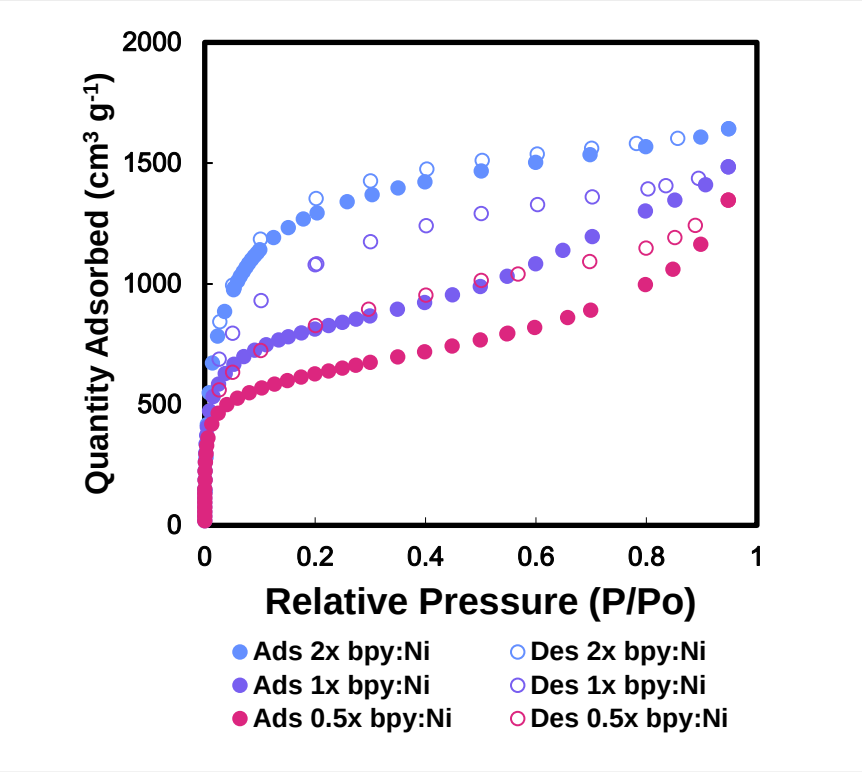

Figure S4. N_2 isotherm at 77 K of **P-1** bipyridine optimization. Both absolute uptake and hysteresis are affected by the bipyridine stoichiometry relative to nickel.

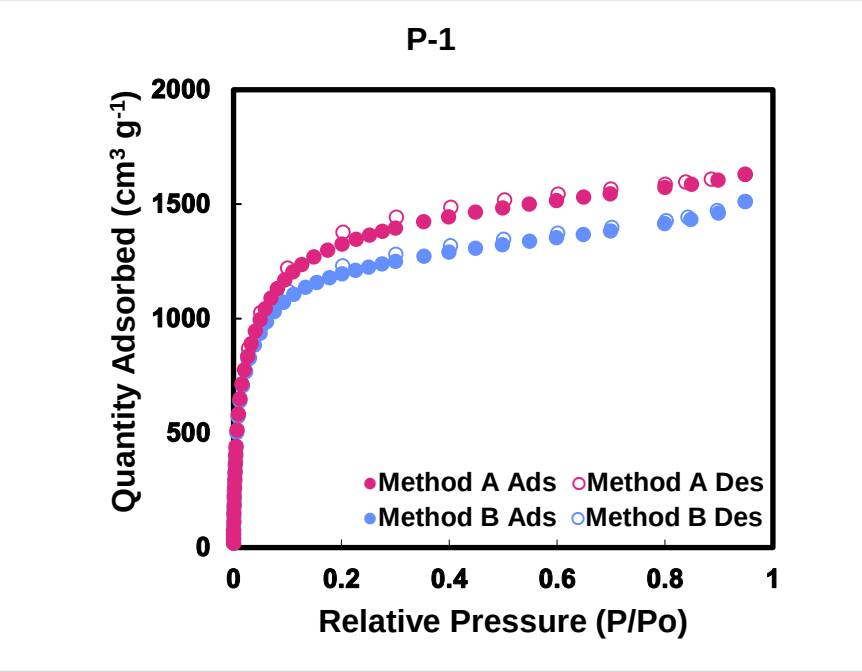

Figure S5. N_2 isotherm of **P-1** at 77 K of **P-1** made from method A and method B.

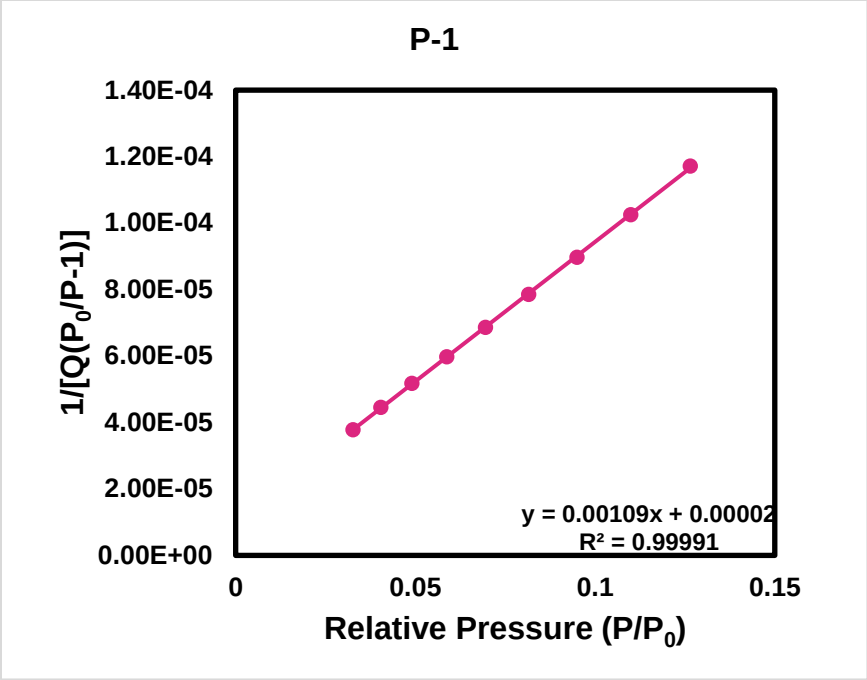

Figure S6. Plot of linear region for the BET equation of **P-1** isotherm made through method A.

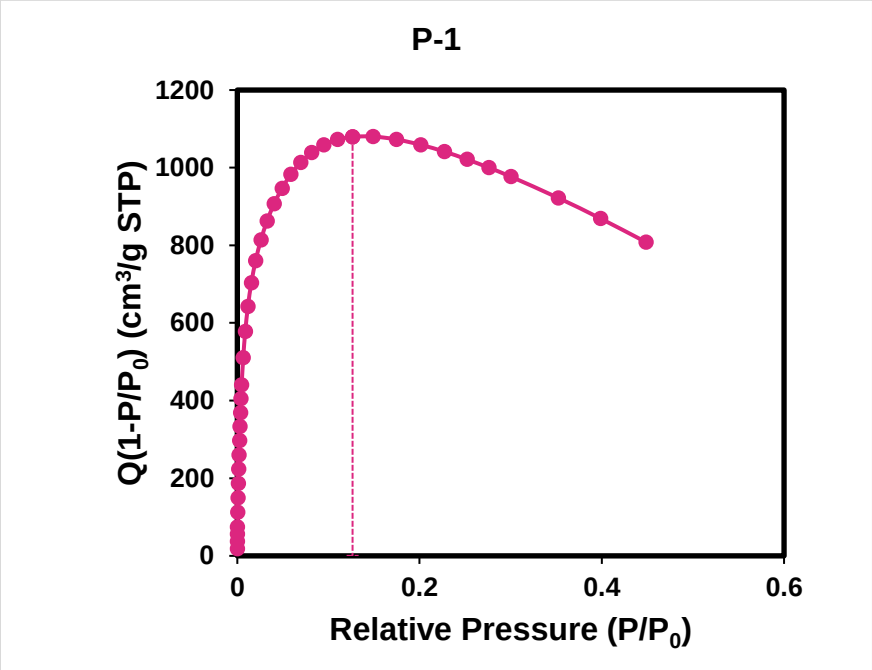

Figure S7. $Q(1-P/P_0)$ vs P/P_0 for **P-1**. The range from the first point to the last point denoted by the dotted line satisfies the first consistency criterion for applying the BET theory.

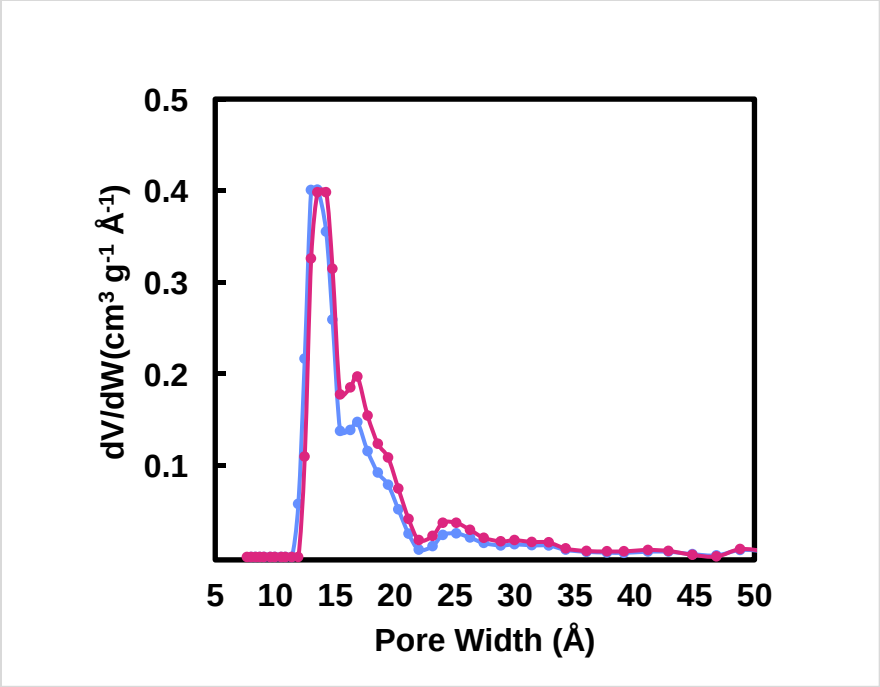

Figure S8. Pore size comparison of **P-1** made through method A (red) and method B (blue). Lines between points are added to guide the eye.

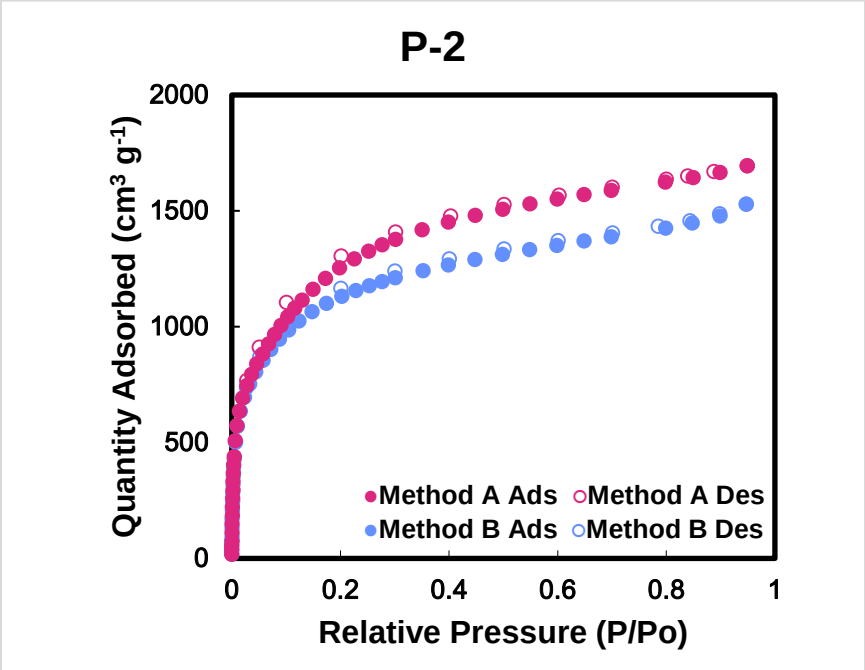

Figure S9. N_2 isotherm of **P-2** at 77 K made through method A (red) and method B (blue)

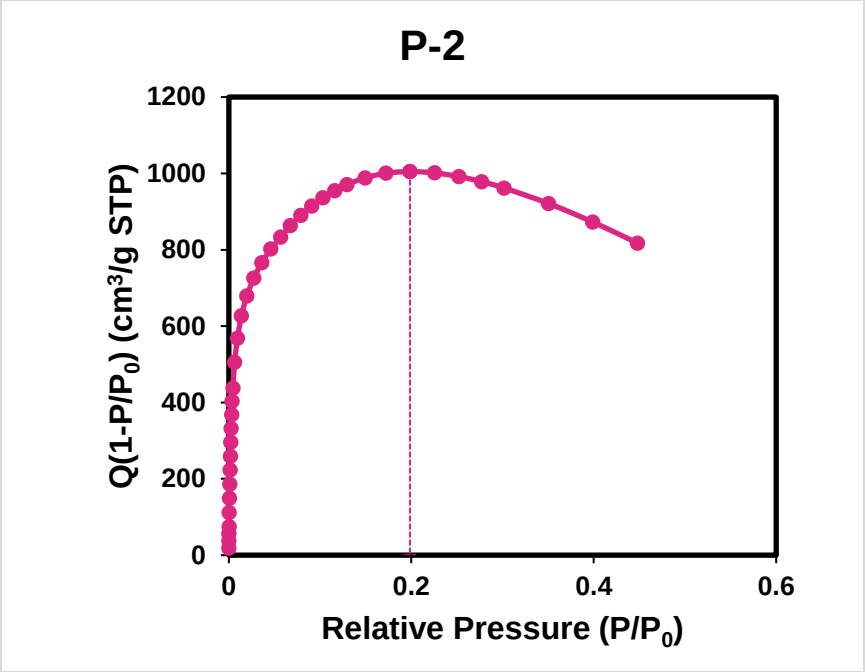

Figure S10. Q(1-P/P_0) vs P/P_0 for **P-2**. The range from the first point to the last point denoted by the dotted line satisfies the first consistency criterion for applying the BET theory.

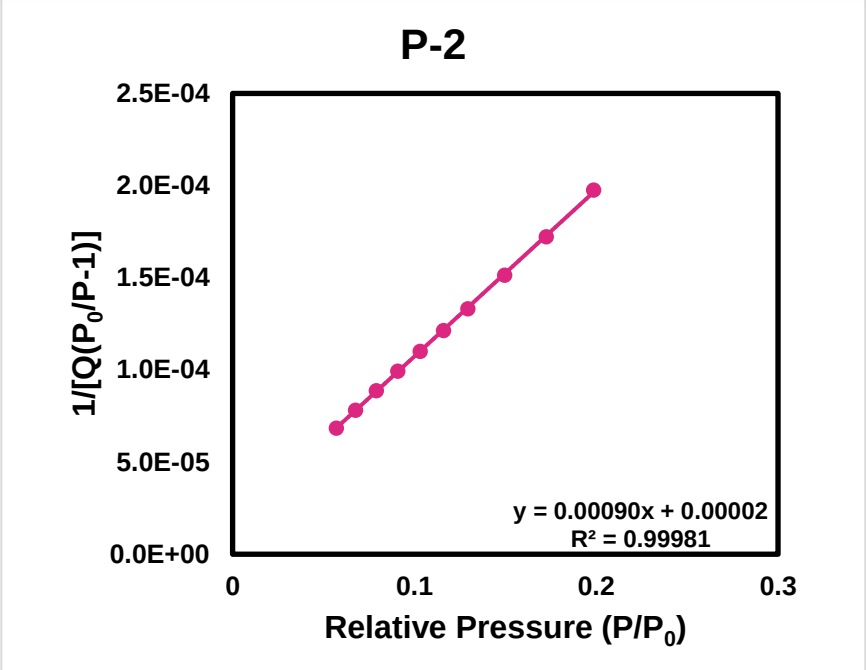

Figure S11. Plot of linear region for the BET equation of **P-2** (method A) isotherm.

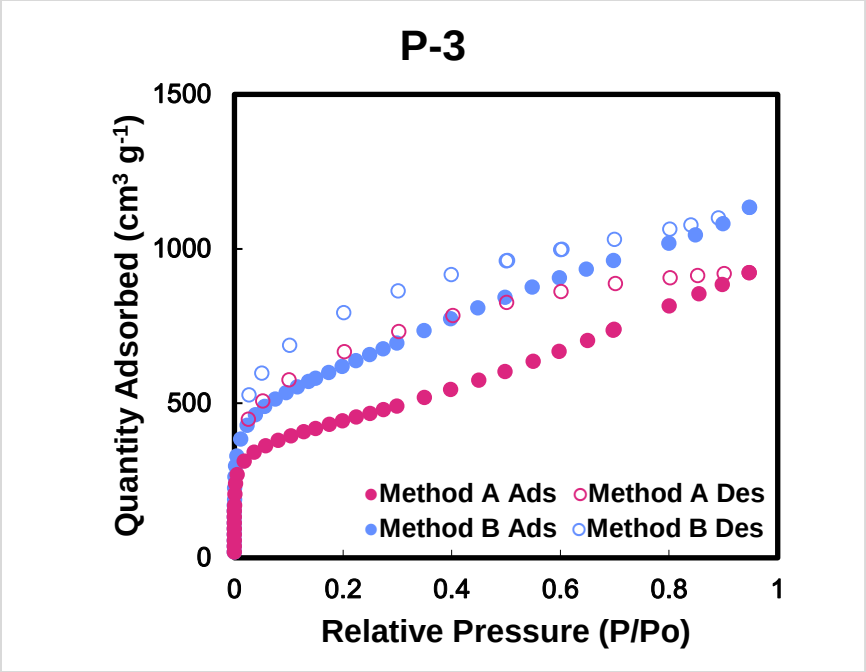

Figure S12. N_2 isotherm of **P-3** at 77 K made through method A (red) and method B (blue)

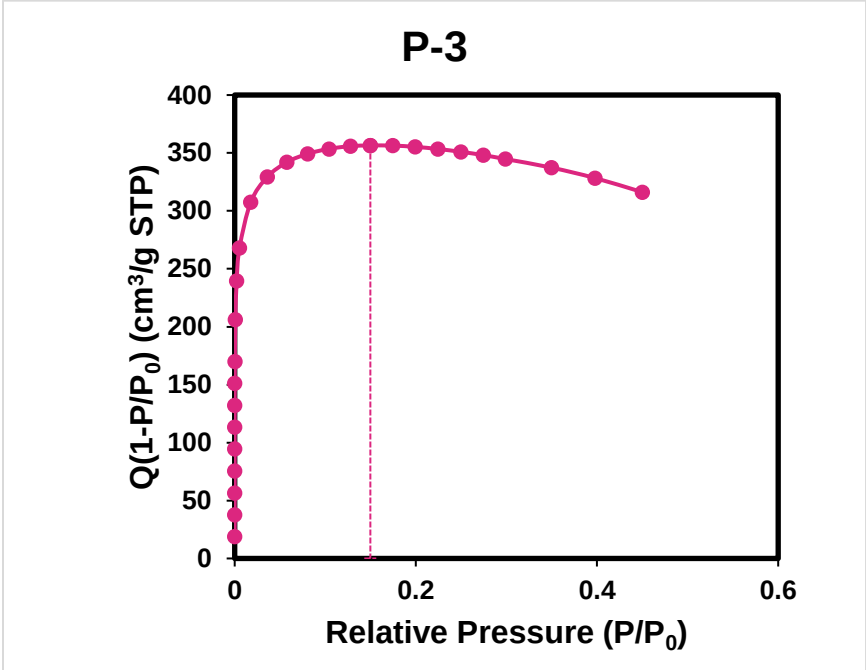

Figure S13. $Q(1-P/P_0)$ vs P/P_0 for **P-3**. The range from the first point to the last point denoted by the dotted line satisfies the first consistency criterion for applying the BET theory.

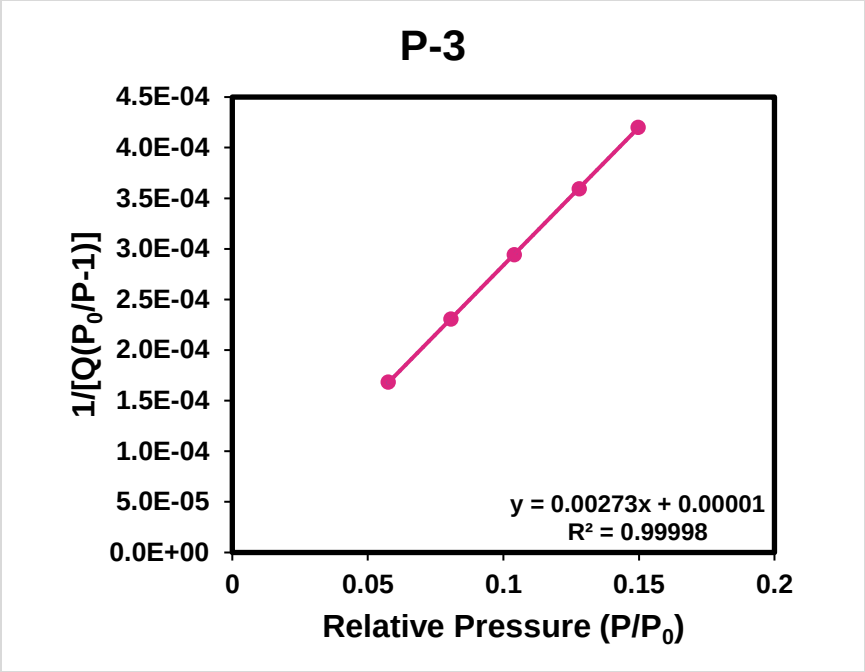

Figure S14. Plot of linear region for the BET equation of **P-3** (method A) isotherm.

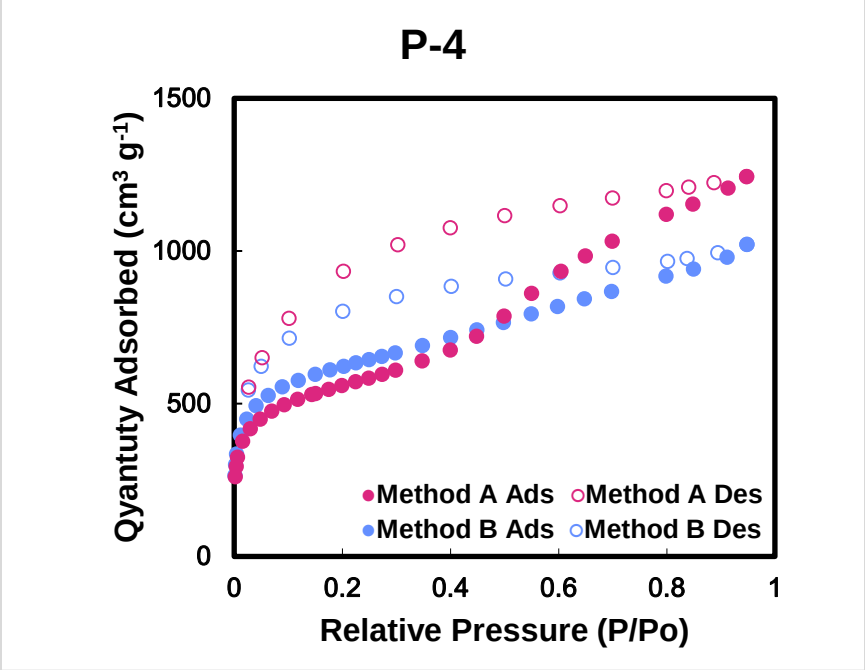

Figure S15. N_2 isotherm of **P-4** at 77 K made through method A (red) and method B (blue)

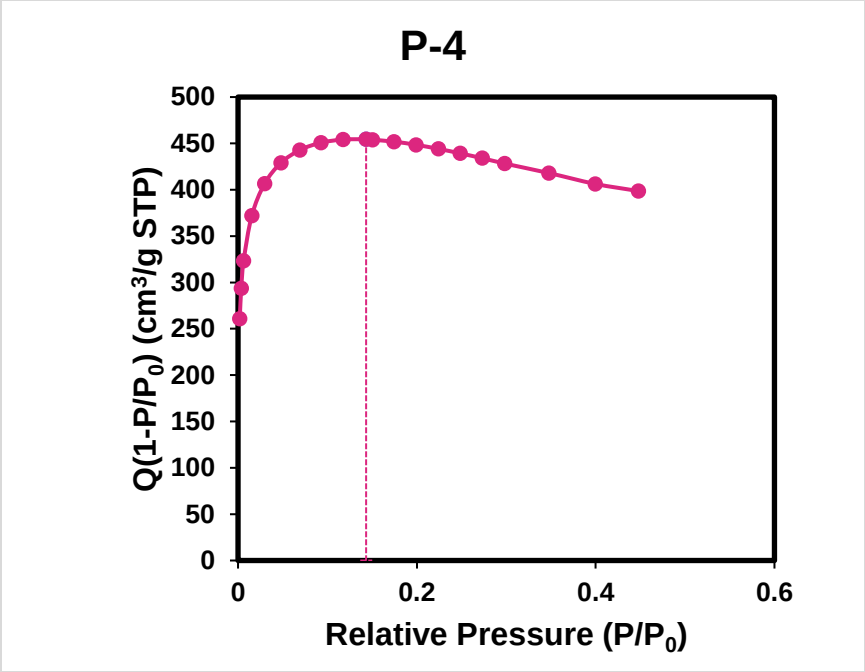

Figure S16. Q(1-P/P_0) vs P/P_0 for **P-4**. The range from the first point to the last point denoted by the dotted line satisfies the first consistency criterion for applying the BET theory.

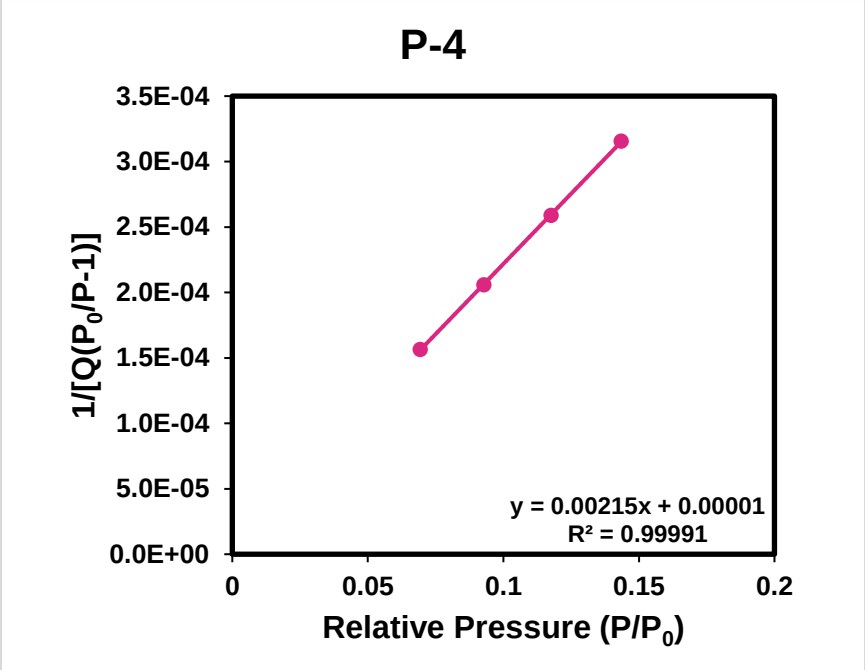

Figure S17. Plot of linear region for the BET equation of **P-4** isotherm.

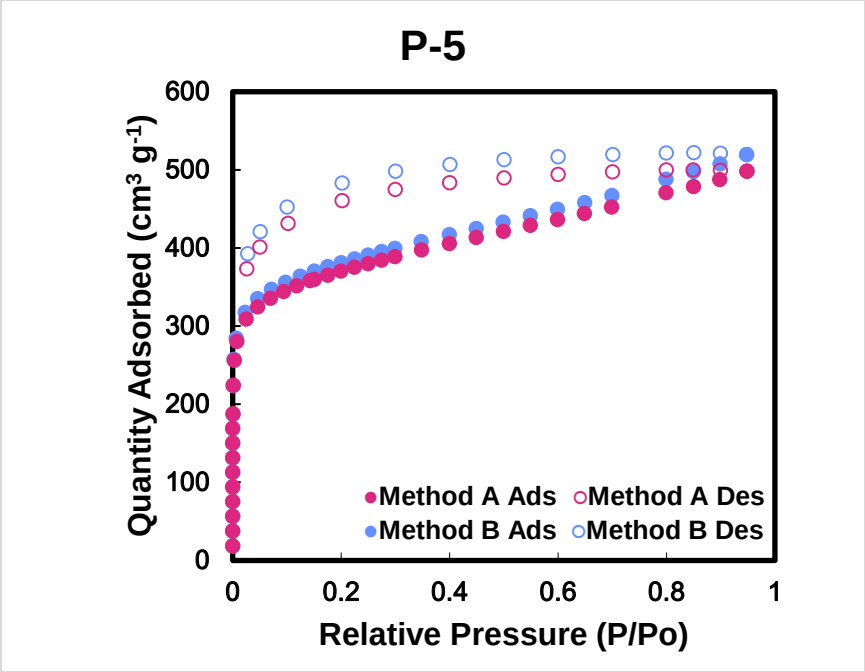

Figure S18. N_2 isotherm of **P-5** at 77 K made through method A (red) and method B (blue)

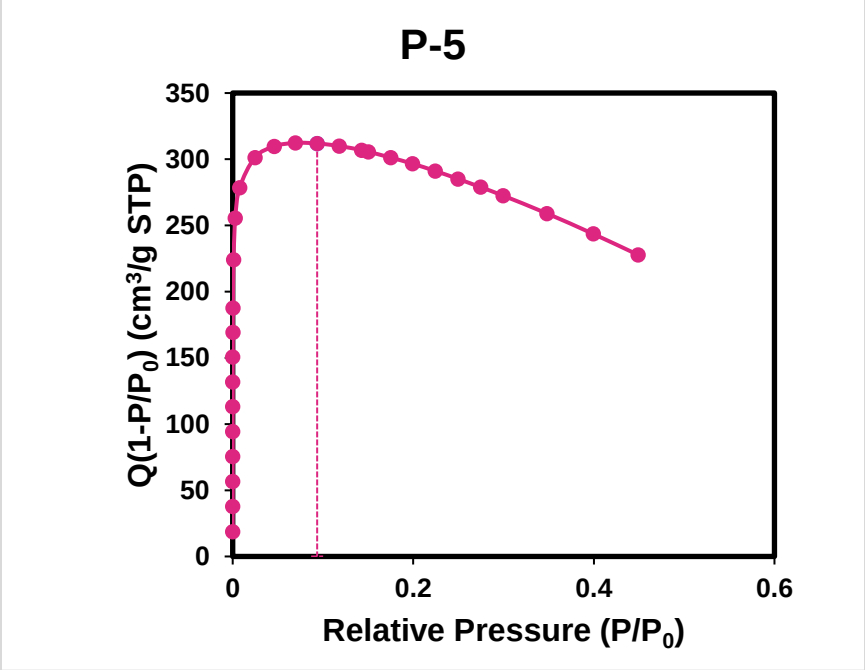

Figure S19. $Q(1-P/P_0)$ vs P/P_0 for **P-5**. The range from the first point to the last point denoted by the dotted line satisfies the first consistency criterion for applying the BET theory.

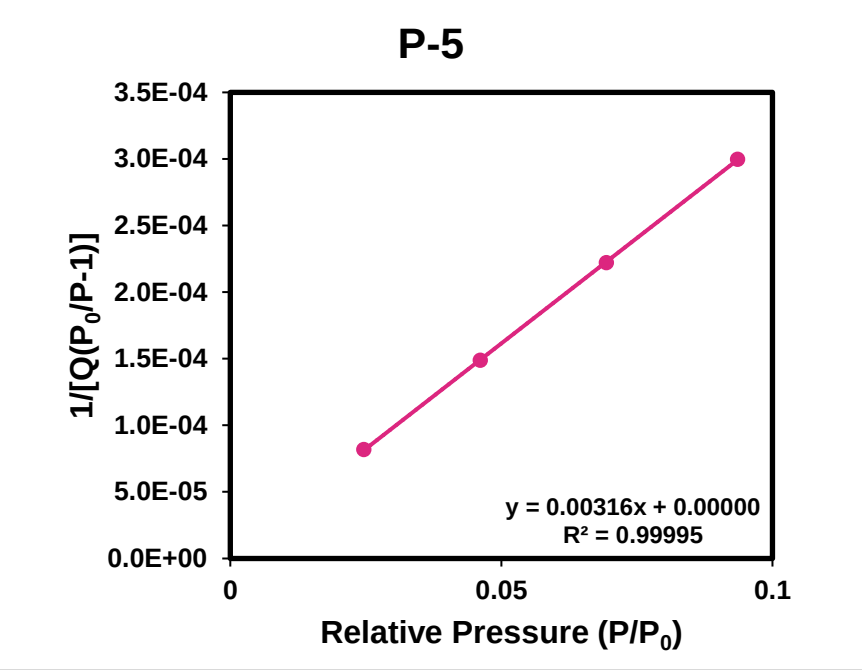

Figure S20. Plot of linear region for the BET equation of **P-5** isotherm.

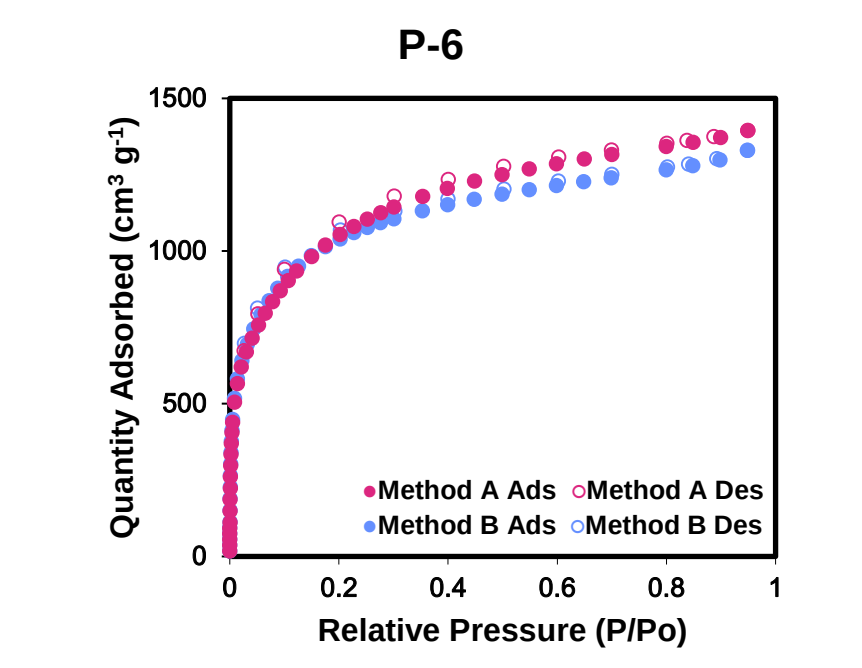

Figure S21. N_2 isotherm of **P-6** at 77 K made through method A (red) and method B (blue)

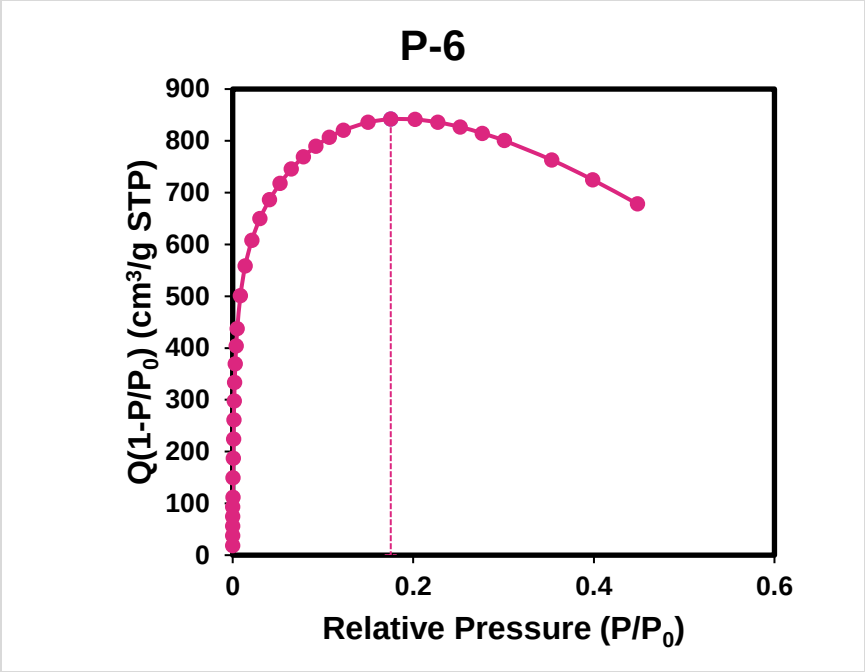

Figure S22. Q(1-P/P_0) vs P/P_0 for **P-6**. The range from the first point to the last point denoted by the dotted line satisfies the first consistency criterion for applying the BET theory.

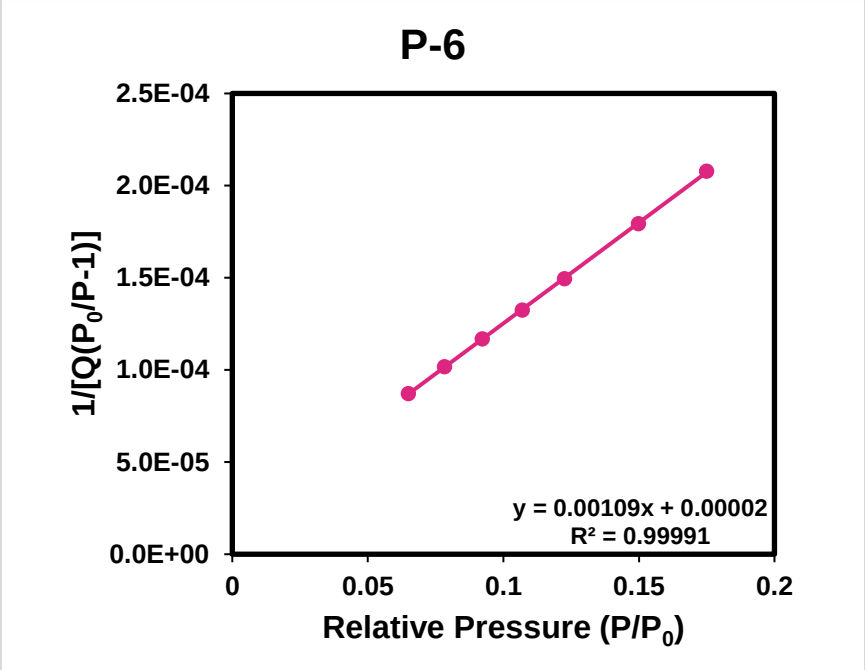

Figure S23. Plot of linear region for the BET equation of **P-6** isotherm.

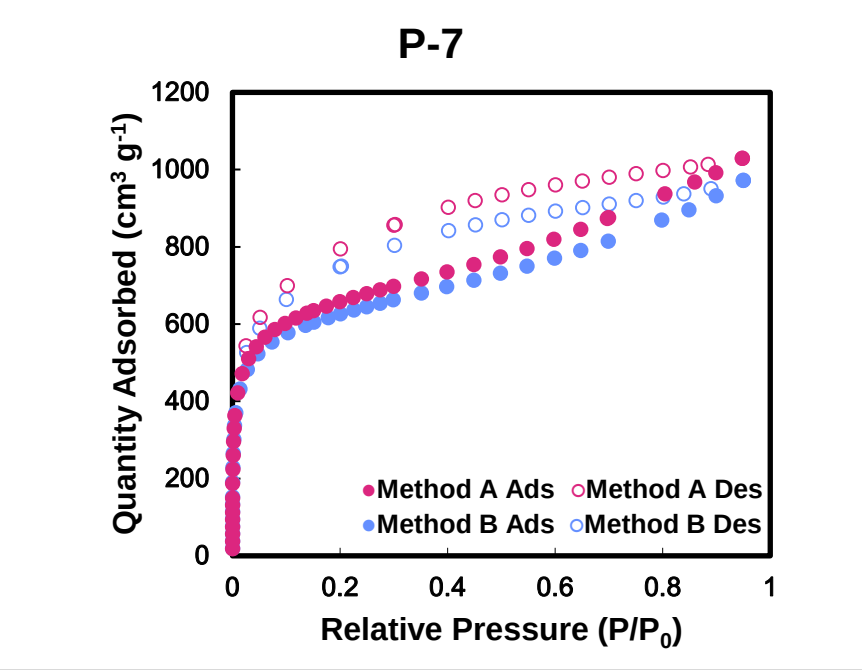

Figure S24. N_2 isotherm of **P-7** at 77 K made through method A (red) and method B (blue)

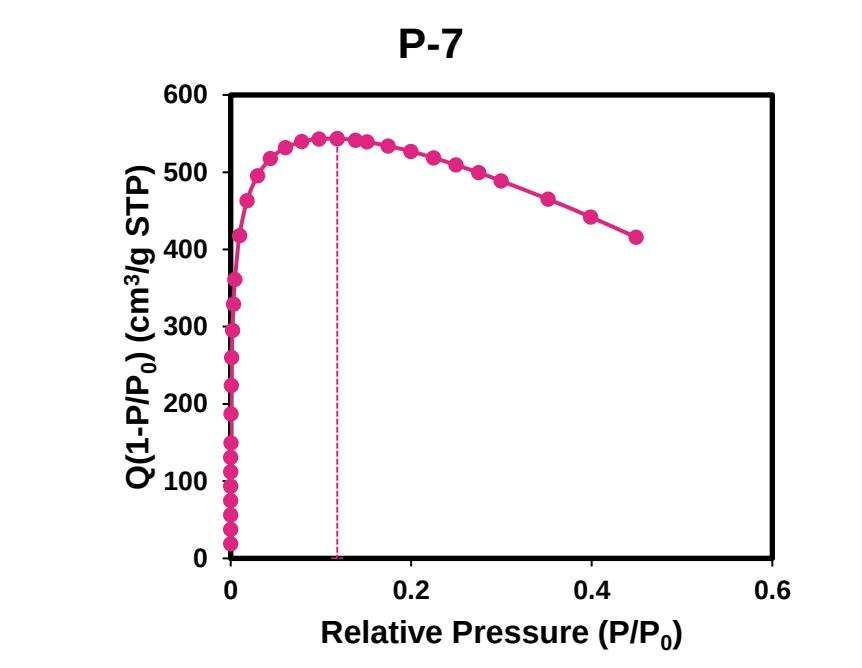

Figure S25. $Q(1-P/P_0)$ vs P/P_0 for **P-7**. The range from the first point to the last point denoted by the dotted line satisfies the first consistency criterion for applying the BET theory.

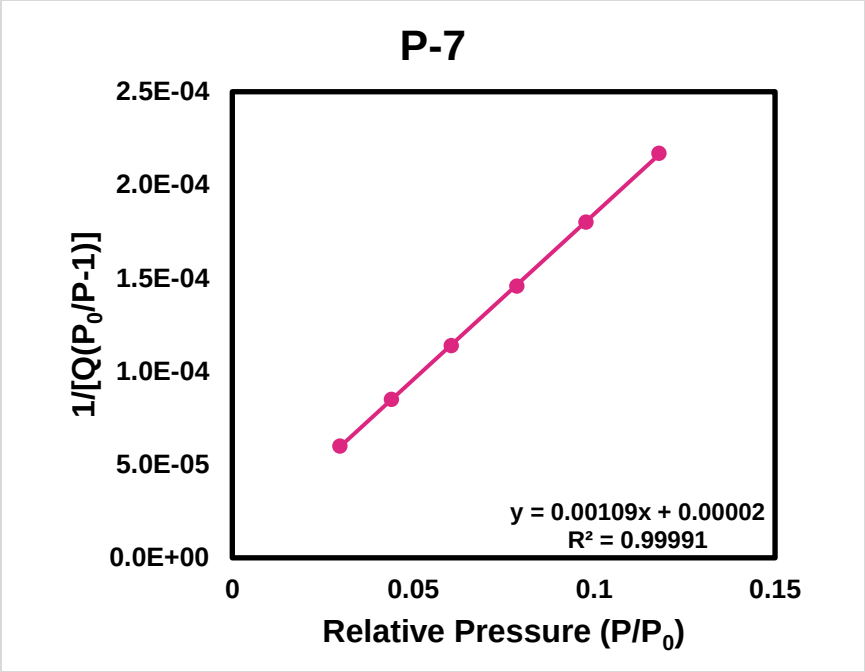

Figure S26. Plot of linear region for the BET equation of **P-7** isotherm.

7.2 CO_2 Isotherms

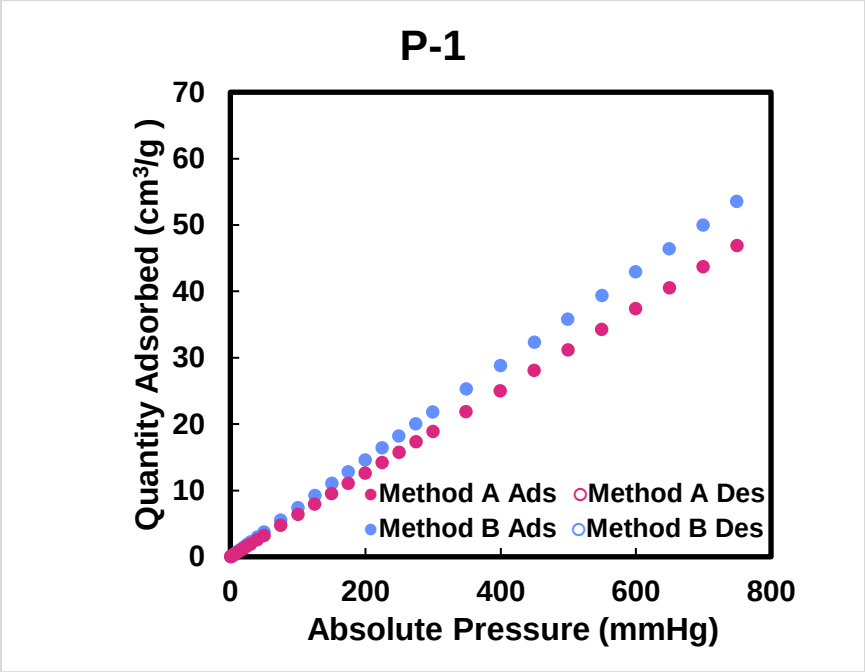

Figure S27. CO_2 isotherm of **P-1** at 273 K made through method A (red) and method B (blue)

7.3 Elemental Analysis Data

Elemental analyses were conducted by Midwest Microlab in Indianapolis, IN, USA. Given the high carbon content, a combustion aid was used. Though carbon content was consistently low, it was consistently low across both methods in comparable magnitude. Low carbon content by combustion analysis has been noted for porous organic polymers by elemental analysis before[15,17]. We have not been able to reproduce literature reports of matching theoretical/experimental elemental analyses for **P-1** even when following other protocols with $Ni(COD)_2$.

Table S3. Elemental analysis results for synthesized PAFs

	Method	P1 [exp/calc]	P-2[a] [exp/calc]	P-3[a] [exp/calc]	P-4[a] [exp/calc]	P-5[a] [exp/calc]	P-6[a] [exp/calc]	P-7 [exp/calc]
C%	A	91.03/94.90	84.66/86.70	93.17/96.13	94.31/95.02	82.52/88.69	82.60/85.67	88.14/93.54
	B	89.00/94.90	83.56/86.70	92.49/96.13	87.31/95.02	77.00/88.69	86.70/85.67	88.16/93.54
	C	90.92/94.90	N/A	N/A	N/A	N/A	N/A	N/A
H%	A	5.14/5.10	5.12/4.85	4.77/3.87	5.37/4.98	5.29/5.09	5.10/4.79	6.5/6.46
	B	4.89/5.10	5.02/4.85	4.46/3.87	5.18/4.98	5.12/5.09	5.19/4.79	6.68/6.46
	C	4.94/5.10	N/A	N/A	N/A	N/A	N/A	N/A
N%	A	0.42/0.00	0.00/0.00	0.00/0.00	0.00/0.00	0.00/0.00	0.00/0.00	0.72/0.00
	B	0.31/0.00	0.00/0.00	0.00/0.00	0.00/0.00	0.00/0.00	0.00/0.00	0.93/0.00
	C	0.37/0.00	N/A	N/A	N/A	N/A	N/A	N/A

[a] Combustion aid used.

7.4 TGA

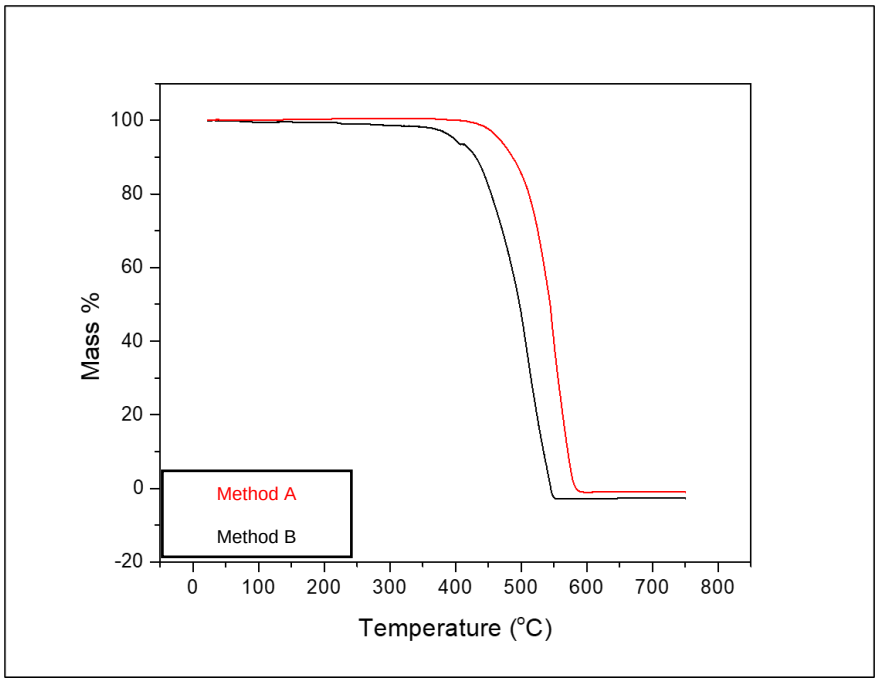

Figure S28. TGA plots of **P-1** made by method A and method B

7.5 PXRD

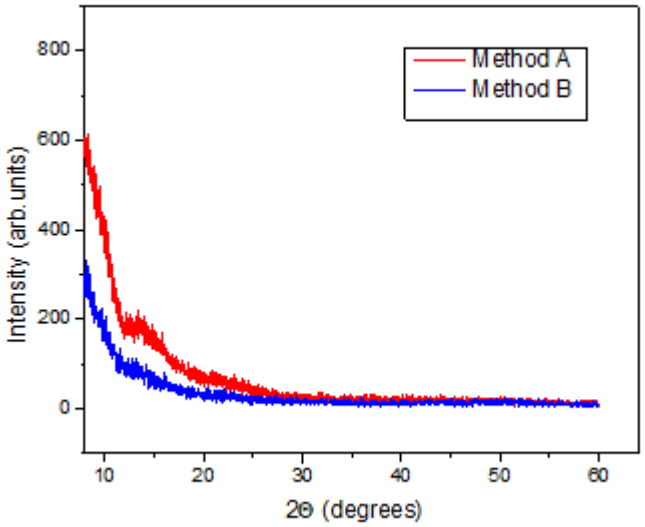

Figure S29. PXRD patterns of **P-1** made by method A and method B

7.6 SEM Images

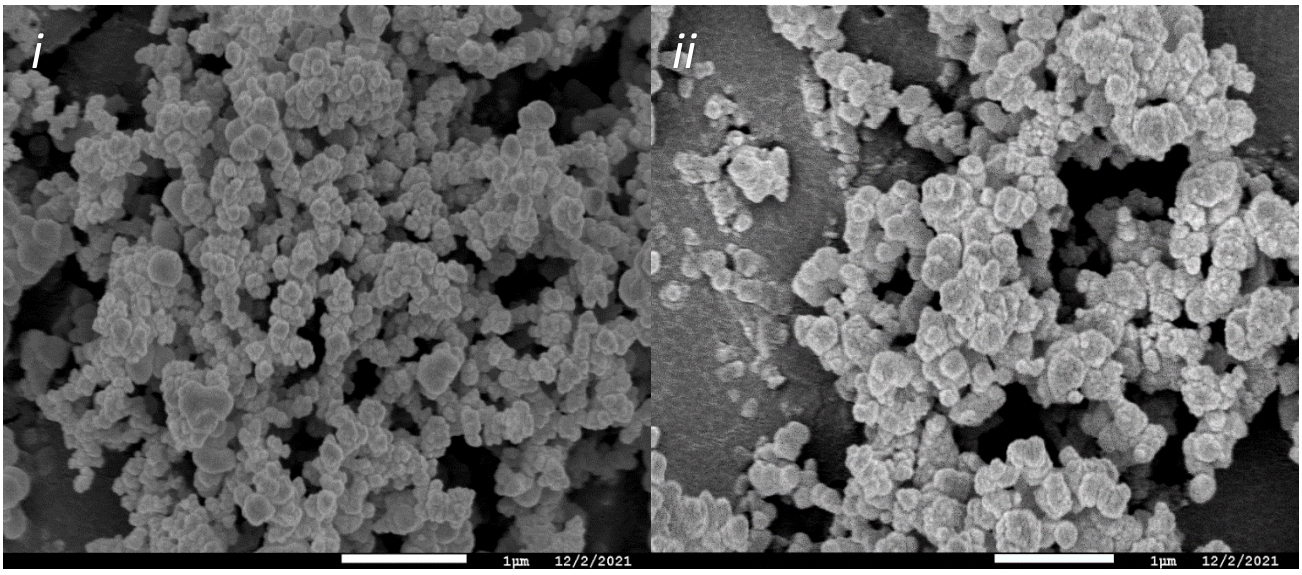

Figure S30. SEM Micrographs of **P-1** made by method A(*i*) and method B (*ii*)

7.7 NMR Spectra

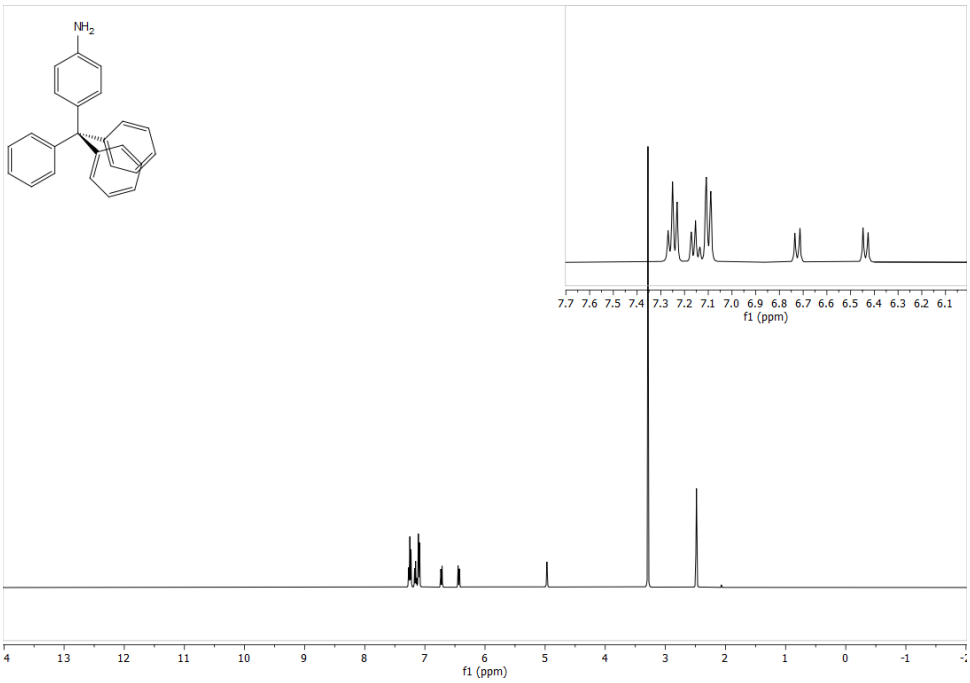

Figure S31. ^{1}H NMR of 4-tritylaniline in $(CD_3)_2SO$ 23 °C

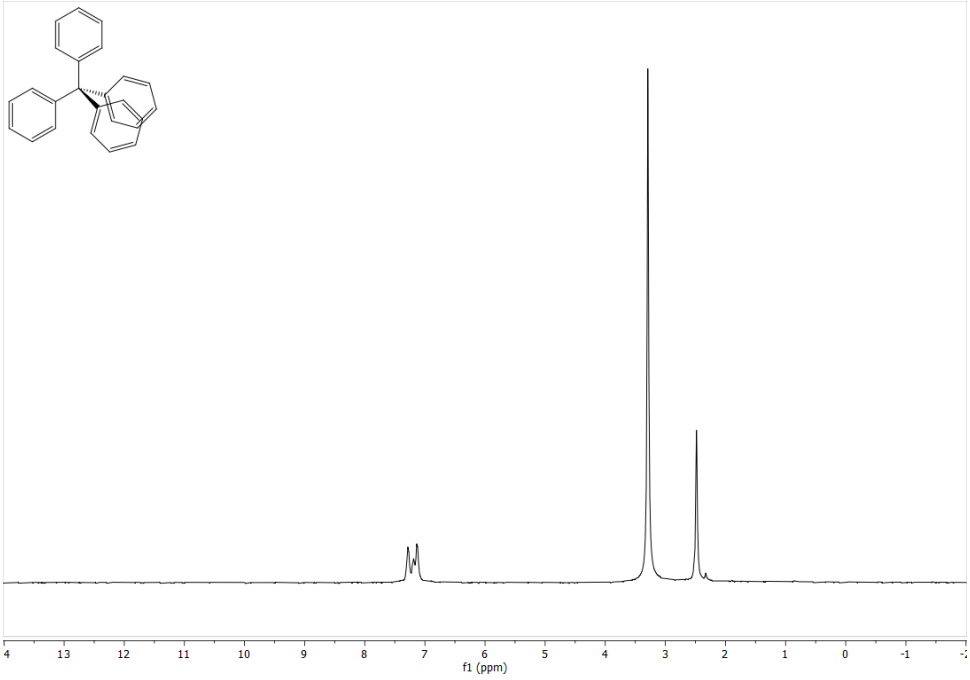

Figure S32. ^{1}H NMR of tetraphenylmethane in $(CD_3)_2SO$ 23 °C

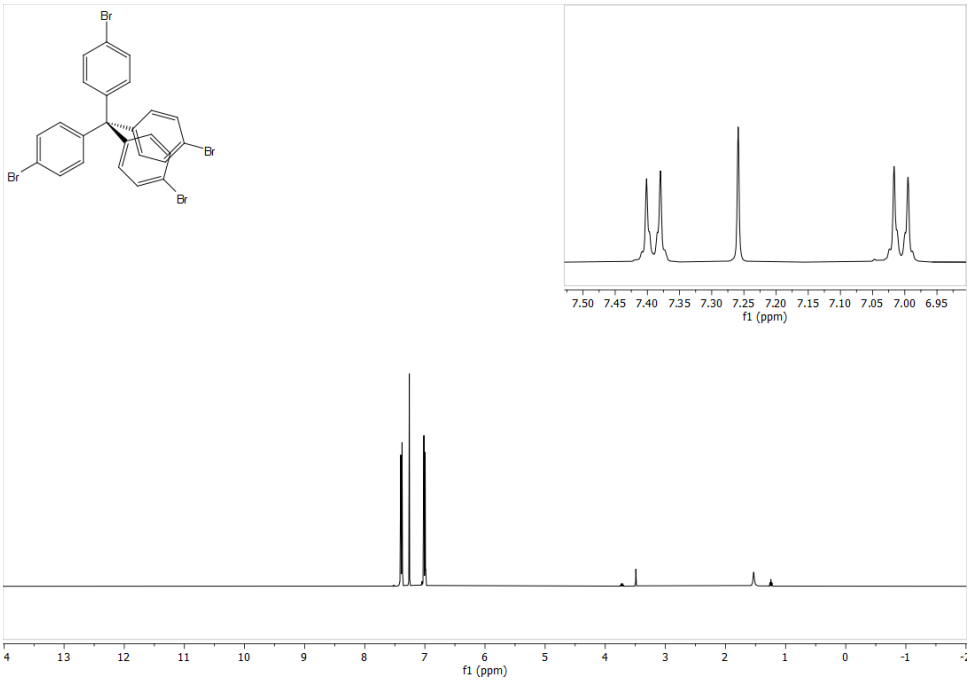

Figure S33. ^{1}H NMR of tetrakis(4-bromophenyl)methane (**M-1**) in $CDCl_3$ at 23 °C

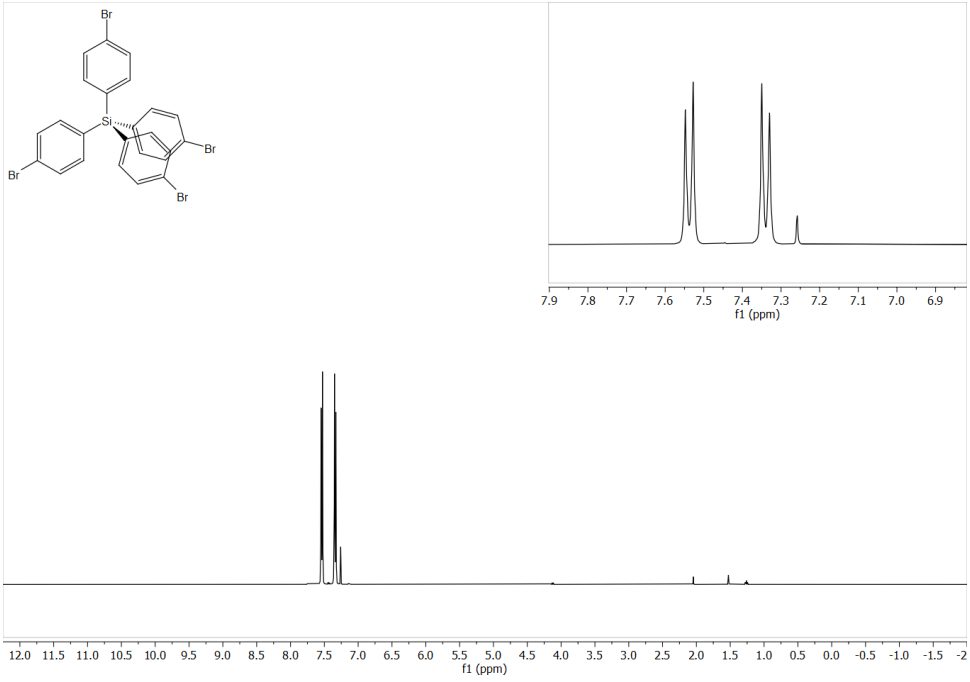

Figure S34. ^{1}H NMR of tetrakis(4-bromophenyl)silane (**M-2**) in $CDCl_3$ at 23 °C

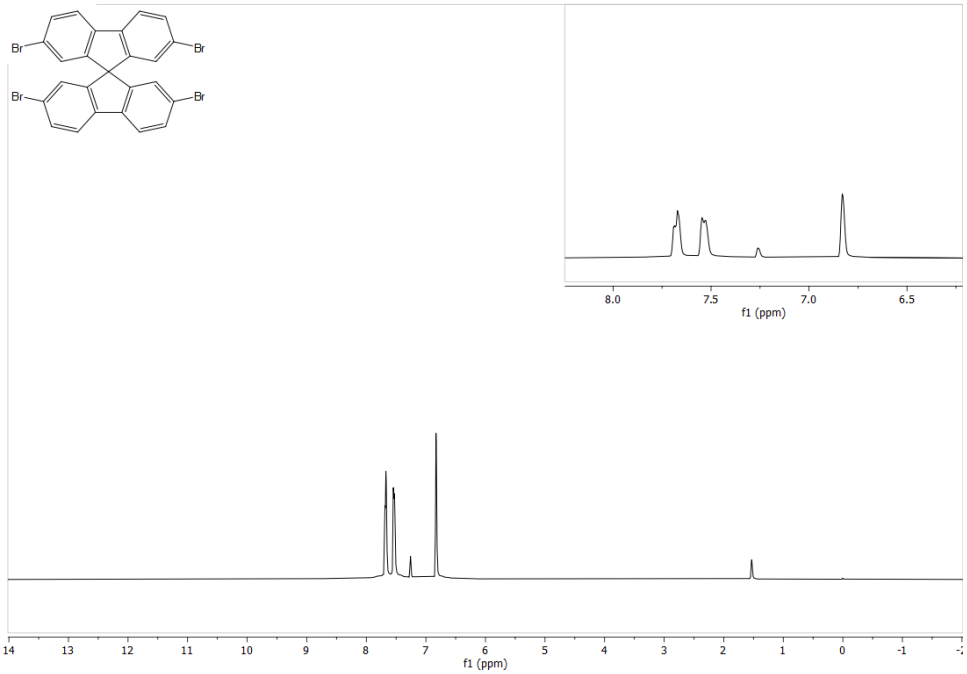

Figure S35. ^{1}H NMR of 2,2',7,7'-tetrabromo-9,9'-spirobi[fluorene] (**M-3**) in $CDCl_3$ at 23 °C

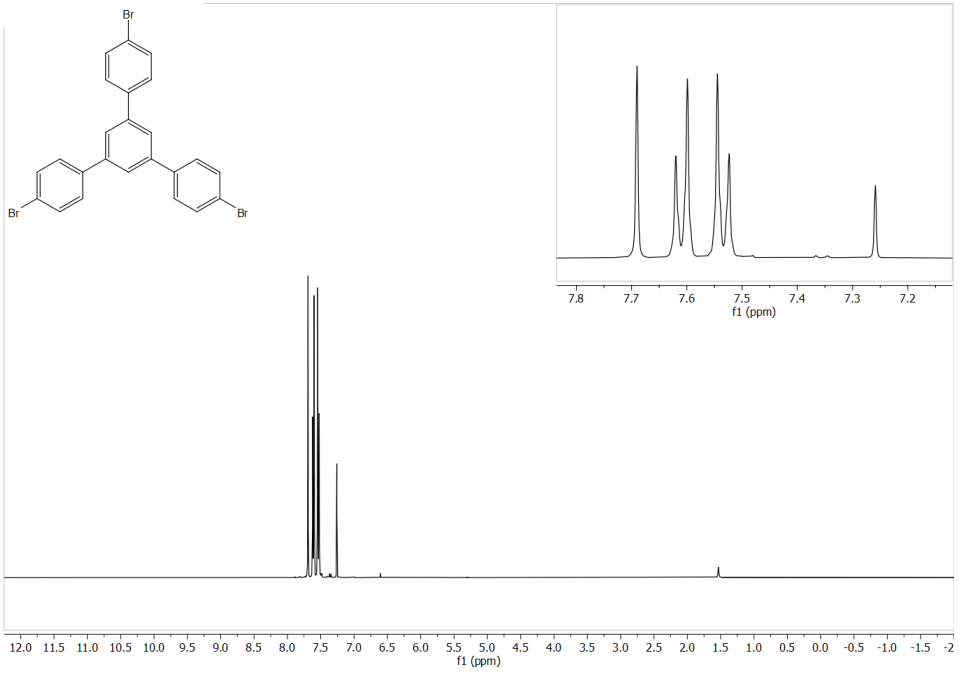

Figure S36. ^{1}H NMR of tris(4-bromophenyl)benzene (**M-4**) in $CDCl_3$ at 23 °C

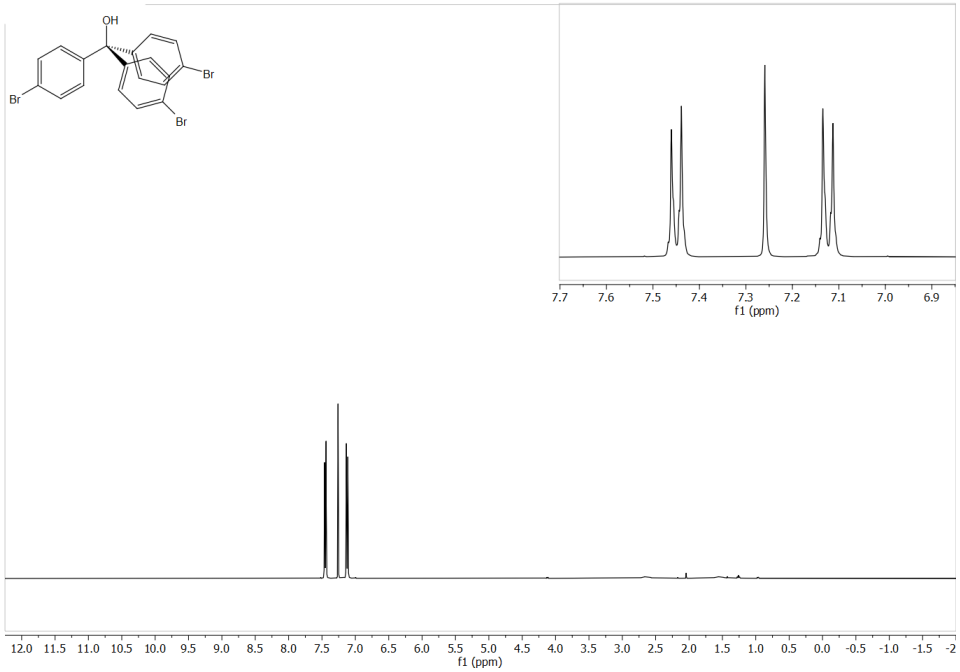

Figure S37. ^{1}H NMR of tris(4-bromophenyl)methanol (**M-5**) in $CDCl_3$ at 23 °C

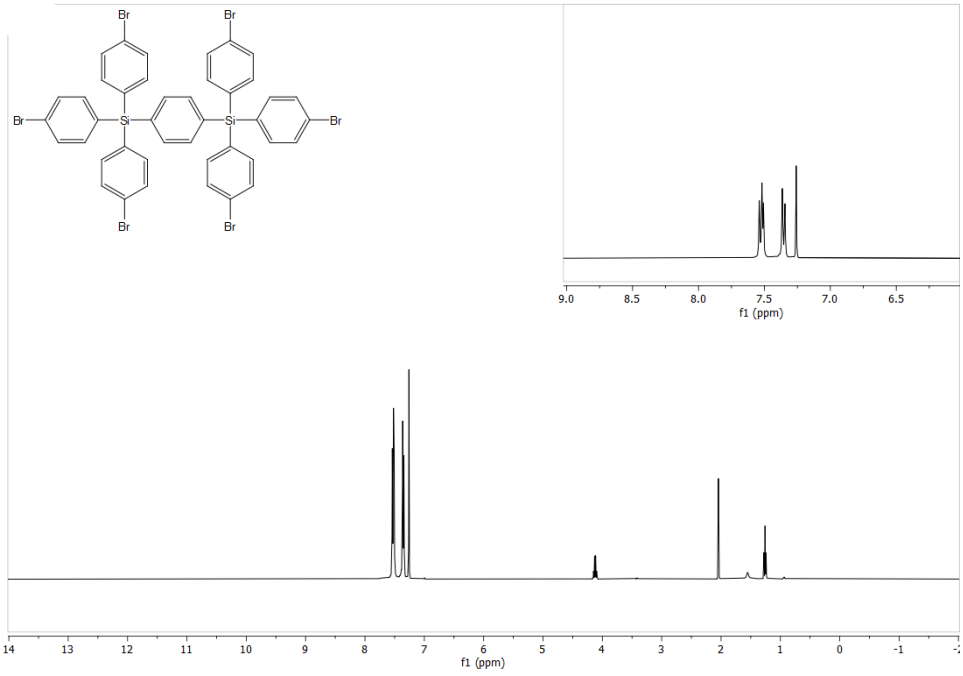

Figure S38. ^{1}H NMR of 1,4-bis(tris(4-bromophenyl)silyl)benzene (**M-6**) in $CDCl_3$ at 23 °C

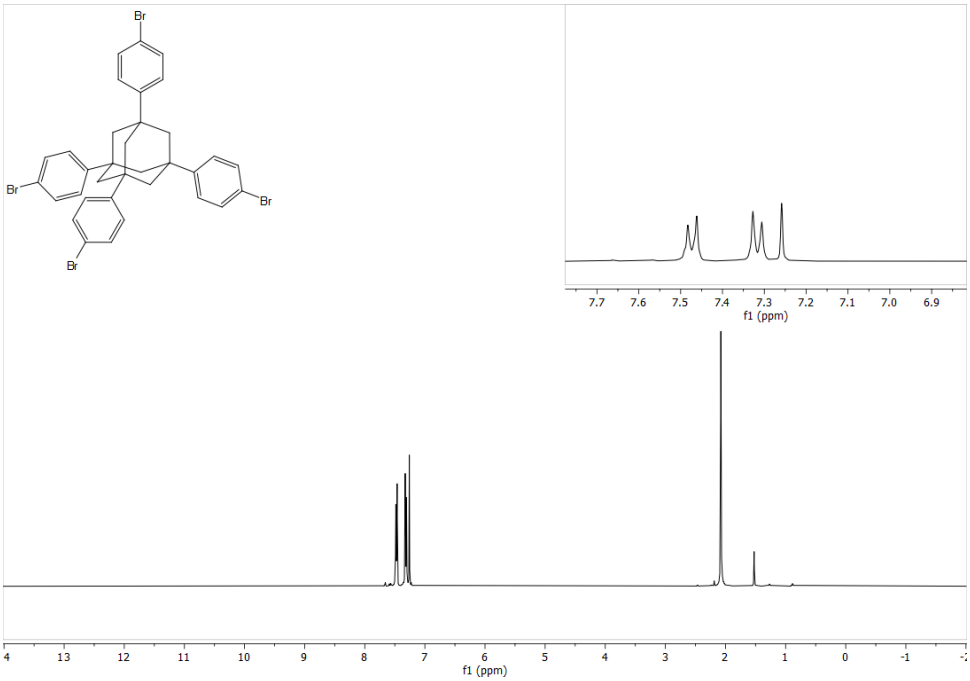

Figure S39. ^{1}H NMR of tetrakis(4-bromophenyl)adamantane (**M-7**) in $CDCl_3$ at 23 °C

7.8 FTIR Spectra

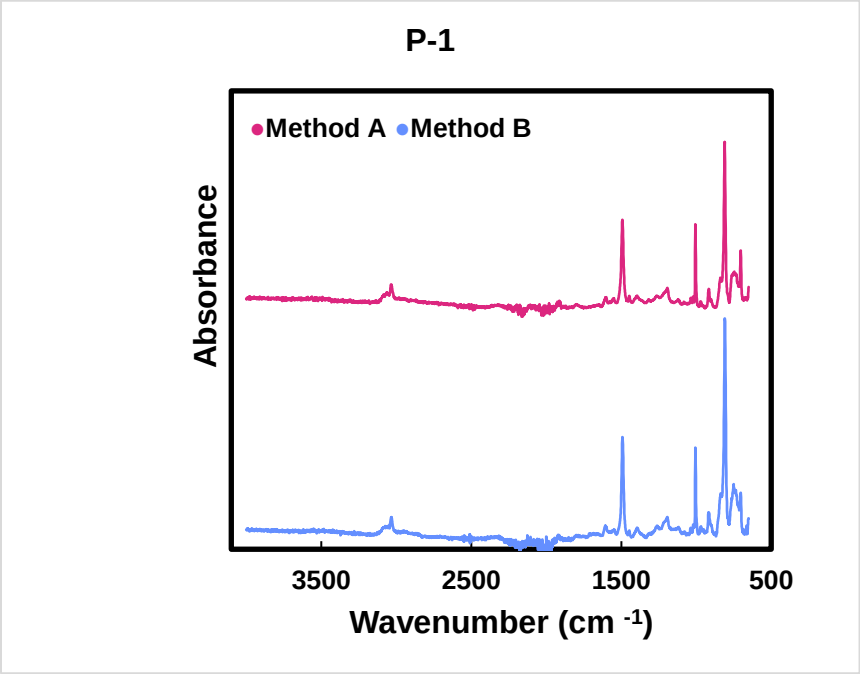

Figure S40. FTIR spectra of **P-1** made through method A and method B

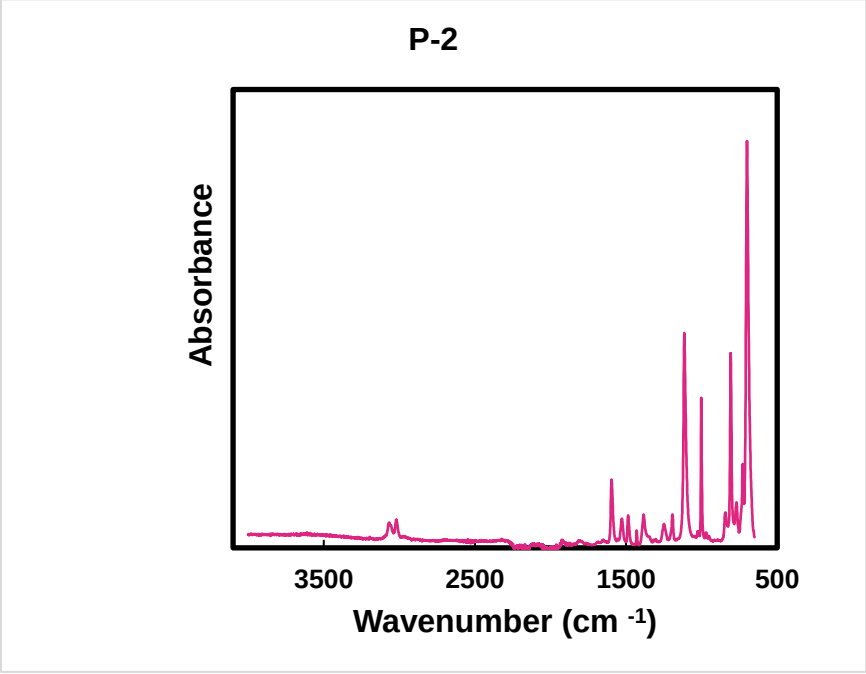

Figure S41. FTIR spectra of **P-2** made through method A.

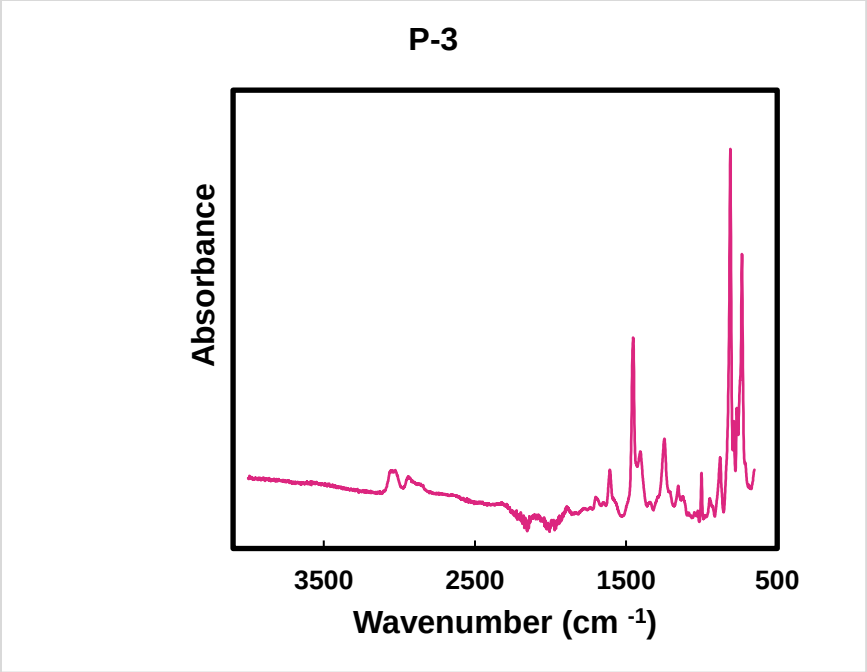

Figure S42. FTIR spectra of **P-3** made through method A.

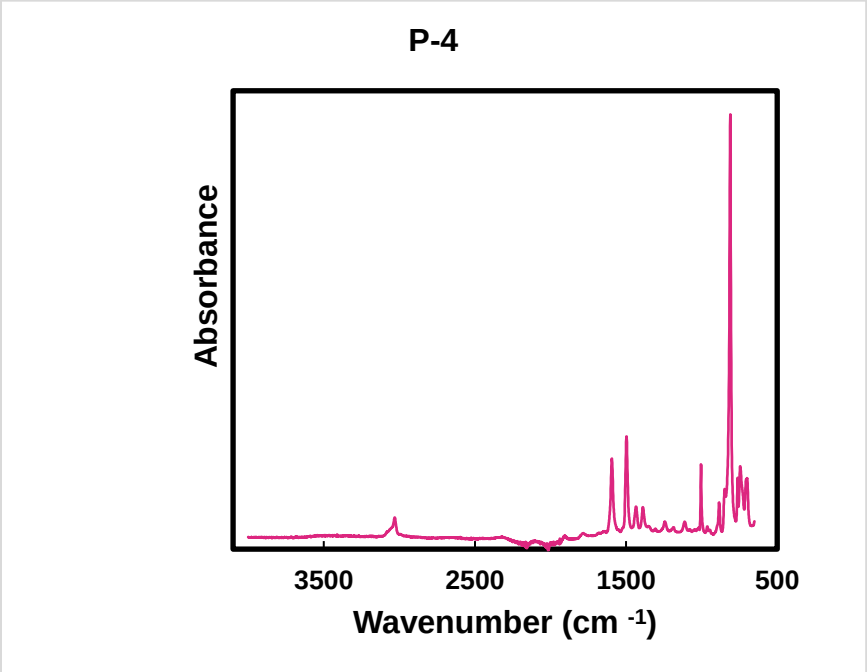

Figure S43. FTIR spectra of **P-4** made through method A.

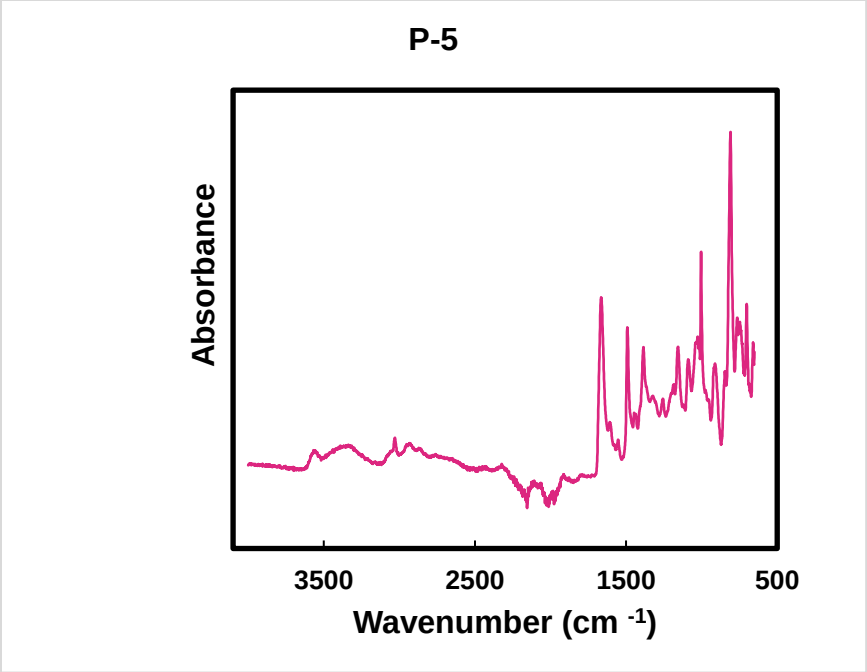

Figure S44. FTIR spectra of **P-5** made through method A.

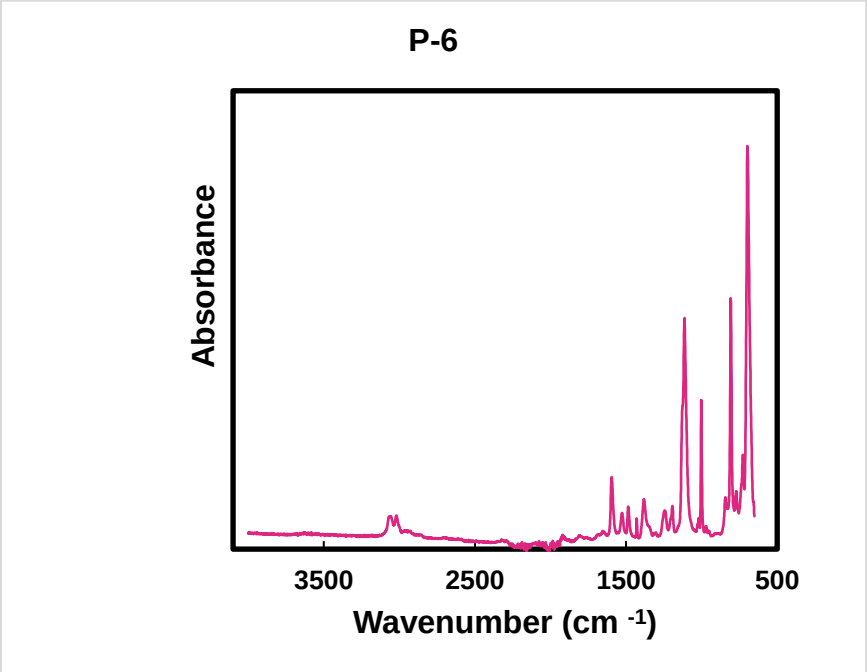

Figure S45. FTIR spectra of **P-6** made through method A.

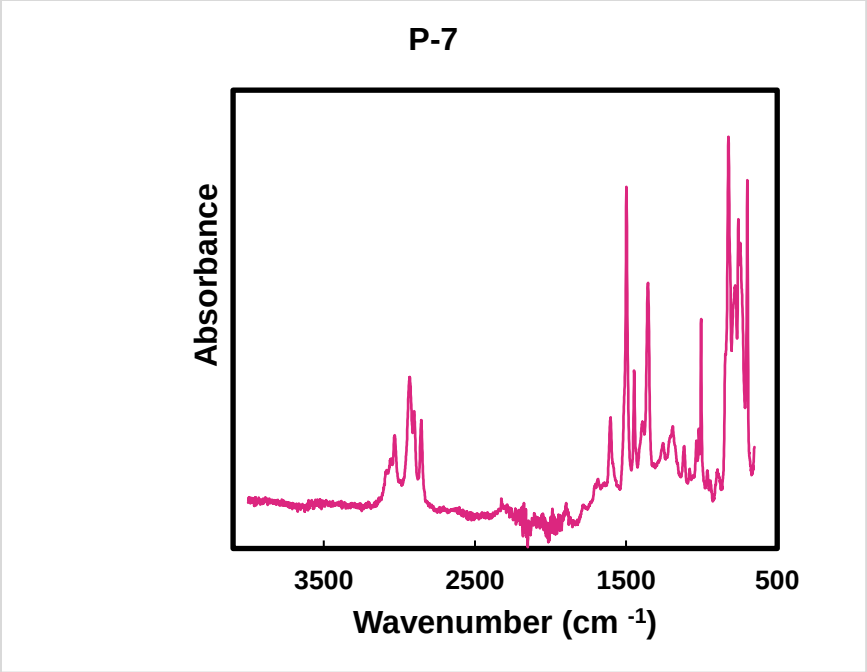

Figure S46. FTIR spectra of **P-7** made through method A

References

(1) Picotin, G.; Miginiac, P. Activation of Zinc by Trimethylchlorosilane. An Improved Procedure for the Preparation of .Beta.-Hydroxy Esters from Ethyl Bromoacetate and Aldehydes or Ketones (Reformatsky Reaction). *J. Org. Chem.* **1987**, *52* (21), 4796–4798. https://doi.org/10.1021/jo00230a029.

(2) Ratsch, M.; Ye, C.; Yang, Y.; Zhang, A.; Evans, A. M.; Börjesson, K. All-Carbon-Linked Continuous Three-Dimensional Porous Aromatic Framework Films with Nanometer-Precise Controllable Thickness. *J. Am. Chem. Soc.* **2020**, *142* (14), 6548–6553. https://doi.org/10.1021/jacs.9b10884.

(3) Urzúa, J. I.; Torneiro, M. Divergent Synthesis of Porous Tetraphenylmethane Dendrimers. *J. Org. Chem.* **2017**, *82* (24), 13231–13238. https://doi.org/10.1021/acs.joc.7b02302.

(4) Verde-Sesto, E.; Pintado-Sierra, M.; Corma, A.; Maya, E. M.; de la Campa, J. G.; Iglesias, M.; Sánchez, F. First Pre-Functionalised Polymeric Aromatic Framework from Mononitrotetrakis(Iodophenyl)Methane and Its Applications. *Chem. - Eur. J.* **2014**, *20* (17), 5111–5120. https://doi.org/10.1002/chem.201304163.

(5) Ma, X. (PhD Thesis, University of Michigan) Synthesis and Functionalization of Three-Dimensional Covalent Organic Frameworks. 234 (https://hdl.handle.net/2027.42/153364.)

(6) Chen, X.; Addicoat, M.; Jin, E.; Zhai, L.; Xu, H.; Huang, N.; Guo, Z.; Liu, L.; Irle, S.; Jiang, D. Locking Covalent Organic Frameworks with Hydrogen Bonds: General and Remarkable Effects on Crystalline Structure, Physical Properties, and Photochemical Activity. *J. Am. Chem. Soc.* **2015**, *137* (9), 3241–3247. https://doi.org/10.1021/ja509602c.

(7) Uptmoor, A. C.; Geyer, F. L.; Rominger, F.; Freudenberg, J.; Bunz, U. H. F. Tetrahedral Tetrakis(*p* -Ethynylphenyl) Group IV Compounds in Microporous Polymers: Effect of Tetrel on Porosity. *ChemPlusChem* **2018**, *83* (5), 448–454. https://doi.org/10.1002/cplu.201800214.

(8) Geyer, F. L.; Rominger, F.; Vogtland, M.; Bunz, U. H. F. Interpenetrated Frameworks with Anisotropic Pore Structures from a Tetrahedral Pyridine Ligand. *Cryst. Growth Des.* **2015**, *15* (7), 3539–3544. https://doi.org/10.1021/acs.cgd.5b00719.

(9) Davies, R. P.; Lickiss, P. D.; Robertson, K.; White, A. J. P. An Organosilicon Hexacarboxylic Acid and Its Use in the Construction of a Novel Metal Organic Framework Isoreticular to MOF-5. *CrystEngComm* **2012**, *14* (3), 758–760. https://doi.org/10.1039/C1CE06091K.

(10) Lu, W.; Yuan, D.; Zhao, D.; Schilling, C. I.; Plietzsch, O.; Muller, T.; Bräse, S.; Guenther, J.; Blümel, J.; Krishna, R.; Li, Z.; Zhou, H.-C. Porous Polymer Networks: Synthesis, Porosity, and Applications in Gas Storage/Separation. *Chem. Mater.* **2010**, *22* (21), 5964–5972. https://doi.org/10.1021/cm1021068.

(11) Uliana, A. A.; Bui, N. T.; Kamcev, J.; Taylor, M. K.; Urban, J. J.; Long, J. R. Ion-Capture Electrodialysis Using Multifunctional Adsorptive Membranes. *Science* **2021**, *372* (6539), 296–299. https://doi.org/10.1126/science.abf5991.

(12) Ben, T.; Pei, C.; Zhang, D.; Xu, J.; Deng, F.; Jing, X.; Qiu, S. Gas Storage in Porous Aromatic Frameworks (PAFs). *Energy Environ. Sci.* **2011**, *4* (10), 3991. https://doi.org/10.1039/c1ee01222c.

(13) Nesmelov, A.; Lee, D.; Bejger, C.; Kocherga, M.; Lyles, Z.; Greenier, M. K.; Vitallo, A. A.; Kaouk, G.; Jones, D. S.; Schmedake, T. A. Accessing New Microporous Polyspirobifluorenes *via* a C/Si Switch. *Chem. Commun.* **2020**, *56* (68), 9846–9849. https://doi.org/10.1039/D0CC02767G.

(14) Ren, H.; Ben, T.; Sun, F.; Guo, M.; Jing, X.; Ma, H.; Cai, K.; Qiu, S.; Zhu, G. Synthesis of a Porous Aromatic Framework for Adsorbing Organic Pollutants Application. *J. Mater. Chem.* **2011**, *21* (28), 10348. https://doi.org/10.1039/c1jm11307k.

(15) Perego, J.; Piga, D.; Bracco, S.; Sozzani, P.; Comotti, A. Expandable Porous Organic Frameworks with Built-in Amino and Hydroxyl Functions for CO_2 and CH_4 Capture. *Chem. Commun.* **2018**, *54* (67), 9321–9324. https://doi.org/10.1039/C8CC03951H.
(16) Li, M.; Ren, H.; Sun, F.; Tian, Y.; Zhu, Y.; Li, J.; Mu, X.; Xu, J.; Deng, F.; Zhu, G. Construction of Porous Aromatic Frameworks with Exceptional Porosity via Building Unit Engineering. *Adv. Mater.* **2018**, *30* (43), 1804169. https://doi.org/10.1002/adma.201804169.
(17) Yuan, D.; Lu, W.; Zhao, D.; Zhou, H.-C. Highly Stable Porous Polymer Networks with Exceptionally High Gas-Uptake Capacities. *Adv. Mater.* **2011**, *23* (32), 3723–3725. https://doi.org/10.1002/adma.201101759.